وزارة التعليم العالي والبحث العلمي

BADJI MOKHTAR –ANNABA UNIVERSITY
UNIVERSITE BADJI MOKHTAR– ANNABA

جامعة باجي مختار - عنابة

Faculty of Science

Year: 2023/2024

Department of Mathematics
Mathematical Modeling and Numerical Simulation Laboratory

THESIS

Presented with a view to obtaining the doctorate degree

ENTITLED

MATHEMATICAL AND NUMERICAL STUDY OF ENVIRONMENTAL POLLUTION PROBLEMS

In
Applied Mathematics
Speciality
Differential Equations and Applications
By

LACHACHE Mohammed

SUPERVISOR : NOURI Fatma Zohra Prof. U.B.M. ANNABA

In front of the jury

PRESIDENT: Laouar Abdelhamid	Prof.	U.B.M. ANNABA
EXAMINER: Benhamidouche Noureddine	Prof.	UNIV. M'SILA
EXAMINER: Zerrouki Ibtissem	Prof.	U.B.M. ANNABA

دراسة رياضية وعددية لمشاكل التلوث البيئي

ملخص:

في هذه الأطروحة قمنا بدراسة النماذج الرياضية التي تصف حركة الملوثات غير المتفاعلة باستخدام معادلات المياه الضحلة، وبدأنا بدراسة حركة ارتفاع الجريان باستخدام نموذج المياه الضحلة، ولهذه الغاية تم استخدام حل الموجة المتحركة لإظهار النتائج النظرية من خلال نظريات النقطة الثابتة لشودر وبناخ. وفي النموذج الثاني، أضفنا معادلة نقل لإجراء تحليل انتشار الملوثات. وفي الجزء الثالث من عملنا، قمنا بدراسة نظام مقترن لنظام سانت فينانت المنتظم مع معادلة النقل ليأخذ بعين الاعتبار حركة الملوثات في التدفق، وتقديم نتائج نظرية على موضعه الصحيح، أي أننا نبين الشروط اللازمة والكافية ليكون النموذج المشتق موضوع بشكل جيد. على أساس موثوق في مخطط الفروق المحدودة، قمنا بدراسة تجزئة النماذج المقترحة وتطبيقاتها، لتقديم نتائج عددية وإظهار السلوك الفعال للظواهر.

الكلمات مفتاحية: نظام سانت-فينانت، نموذج المياه الضحلة، معادلة النقل، حلول الموجات المتنقلة، طريقة الفروق المحدودة.

Etude Mathématique et Numérique des Problèmes de Pollution Environnementale

Résumé

Dans cette thèse, nous étudions des modèles mathématiques qui décrivent le mouvement de polluants non réactifs à l'aide d'équations des eaux peu profondes. Nous commençons par étudier le mouvement de la hauteur d'écoulement à l'aide d'un modèle en eaux peu profondes. À cette fin, nous utilisons la solution des ondes progressives pour démontrer des résultats théoriques à travers les théorèmes du point fixe de Schauder et Banach. Dans le deuxième modèle, nous ajoutons une équation de transport pour effectuer une analyse de la propagation des polluants. Dans la troisième partie de notre travail, nous étudions le système couplé d'un système de Saint-Venant régularisé avec l'équation de transport pour prendre en compte le mouvement des polluants dans l'écoulement, en présentant des résultats théoriques sur sa bonne position, c'est-à-dire que nous montrons les conditions nécessaires et suffisantes pour que le modèle dérivé soit bien posé. Sur la base d'un schéma de différences finies fiable, nous examinons la discrétisation des modèles proposés et leurs implémentations, pour fournir des résultats numériques et montrer le comportement effectif des phénomènes.

Mots-clés: système de Saint-Venant, modèle d'eau peu profonde, équation de transport, solutions à ondes progressives, méthode des différences finies.

Mathematical and numerical study of environmental pollution problems

Abstract

In this thesis, we study mathematical models that describe the motion of non-reactive pollutants using shallow water equations. We begin by studying the motion of the flow height using a shallow water model. For this purpose, we utilize the traveling wave solutions to demonstrate theoretical results through Schauder's and Banach's fixed point theorems. In the second model, we add a transport equation to conduct an analysis of pollutant propagation. In the third part of our work, we study the coupled system of a regularized Saint-Venant system together with the transport equation to take into account the motion of pollutants within the flow; presenting theoretical results on its well-posedness, i.e we show the necessary and sufficient conditions for the derived model to be well posed. Based on a reliable finite difference scheme, we examine the discretization of the proposed models and the implementations, to provide numerical results and show the effective behavior of the phenomena.

Keywords: Saint-Venant system, shallow water model, transport equation, traveling wave solutions, finite difference method.

Acknowledgements

Above all, I am grateful to ***Allah****, the Almighty and Wise, who gave me the capacity, persistence, and reasoning abilities to complete my thesis.*

I want to convey my heartfelt appreciation to my supervisor, ***Prof. Fatma Zohra Nouri****, for her invaluable advice, guidance and unwavering encouragement throughout this research.*

I extend my heartfelt thanks to the members of my thesis committee:

Prof. Laouar Abdelhamid*, as president of the jury deserves sincere thanks for agreeing to preside over the jury for the examination and judgment.*

Prof. Benhamidouche Noureddine*, as examiner, without hesitation, has agreed to review and critique this work. He will likely enrich it with his experience as a researcher and educator.*

Prof. Zerrouki Ibtissem*, as examiner, has bestowed upon me the great honor of taking the time to read and evaluate this work.*

Finally, I want to thank my family and friends, Especially ***my parents*** *and* ***my brothers****,* ***Dr. Houssam Lachache*** *and* ***Dr. Abdelhalim Lachache****, for their continuous encouragement and moral support during this scientific track.*

Contents

List of Figures

Introduction

Nowadays, our world is grappling with the critical issue of environmental pollution, a problem that poses a significant and lasting threat to humanity. Pollution comes in various forms, encompassing the air we breathe and the water we drink. This pervasive issue arises when contaminants are introduced, whether through natural processes or human activities.

Organic pollution in surface waters is a pressing concern that demands urgent attention. In 1925 Streeter and Phelps [50] offer valuable insights into the sources of pollution, the mechanisms of pollutant dispersion, and the river's inherent capacity for self-purification. Their research sheds light on the interplay between human activities and environmental health, providing a foundational understanding that informs strategies for water resource management and pollution control.

Our main focus is on addressing the issue of organic pollution in surface waters, with a specific focus on employing mathematical and numerical techniques to analyze a system of partial differential equations that models the distribution of organic pollution in lakes or estuaries.

To approach this challenge, it is essential to understand the motion of water flow and one of the most used models in this context, at least as a first approximation, is the Saint-Venant system, introduced in 1871 [46], while the transport equation provides a framework

for analyzing the movement of pollutants within the water system. By integrating these two equations, we can gain insights into how organic pollutants disperse and impact the dynamics of water flow.

Figure 1 shows the propagation of Pollution in the Water presented as follows:

Figure 1: Water Pollution.

The saint-Venant system (SV-S) is a mathematical model that characterizes the dynamics of fluid flows in rivers and lakes. It was derived by integrating the Navier-Stokes equations [39] to account for situations where the horizontal flow length significantly exceeds the vertical one. This system was formulated by Saint-Venant in 1871 [46] and subsequently, another version was developed by Gerbeau et al. in 2000 [23]. Since then, there has been a growing interest among researchers in exploring and studying the implications and applications of

these equations over the past two decades, for example, see [1], [12], [22] and [52], there are also who studied the regularisation of this model see for example [20], [36] and [45].
Recently, this system has been utilized to model a wide range of scenarios, including environmental pollution. Several numerical methods have been proposed to investigate the behavior of surface flow in SV-S, such as finite differences see for examples [28]. Additionally, for finite element method, we can cite [37], for volume method to [12] and for method of characteristics [29] can be cited.
Numerous researchers have investigated this phenomenon, where the bottom topography non-flat see For example [23] and [43].
In 2008 Mamadou et al [10] derived a shallow water model (SWM) based on certain assumptions, and gave theoretical results for the linear problem. We studied the non-linear of this model theoretically and numerically cited in [33].
Nevertheless, the transportation of pollutants through flows continues to pose a significant threat from both an environmental and industrial perspective. Several authors have also formulated mathematical models for analyzing pollution dispersion; for instance, refer to [16] and [55].
Here, we are focused on studying the connection between the SV-S and the transport equation (T-E), a topic that has garnered significant attention from a multitude of researchers. Many have delved into this area in order to calculate the motion of passive pollutants using the SV-S, see for example [5], [9], [19], [38] and [54].

The uniqueness of our work lies in our proposal, exploration and discussion of new methods which were represented in: First, our investigation of traveling wave forms (refer to [33]). This approach holds great significance in various scientific domains such as computer science, physics, biology, and medicine, as it aids in simplifying complex problems, thereby contributing to their analysis and understanding. Secondly, We use the notion of Gibbs equilibrium to

turn the regularized version of the SV-S with a transport equation into The Boltzmann-type kinetic equations to demonstrate existence and uniqueness of solution.
The present thesis is structured into four separate chapters, as follows.
In the first chapter, we establish the foundation of our study by outlining the mathematical models and reviewing fundamental concepts that are essential for our further exploration; These include the SV-S, the T-E, and the fixed point theorems of Banach and Schauder.

In the second chapter, To illustrate the dynamics of flow height motion, we investigate a nonlinear SWM. We prove theoretical results based on the traveling wave solutions trough the fixed point theorems of Schauder and Banach. For numerical experiments, we examine the two models which are the linear and nonlinear models and assess the behavior solutions for the height and the discharge using a finite difference method.
The results obtained in this chapter have been published in a globally renowned journal cited in [33].

In the third chapter, we examine a non linear SWM coupled with T-E to describe the pollution propagation by conducting a mathematical analysis to establish the well-posedness of the model, utilizing traveling wave solutions to support our findings. Through Schauder's and Banach's fixed point theorems, we prove the well-possess. For numerical discretisation we examine the proposed model and assess its stability conditions using a finite difference method.
An article presenting the results obtained in this chapter has just been submitted.

In the fourth chapter, We examine an alternate model, which is represented by a distinct version of the SV-S, that describes the movement of a passive pollutant. For this, we take into account a regularization of the SV-S. to which we add a T-E. We present theoretical results on its well posedness. and then, based on a reliable finite difference scheme, we exam-

ine discretisations of the proposed model to provide numerical results and show an effective behavior of the phenomena.

An article presenting the results obtained in this chapter has just been submitted.

Chapter 1

Preliminaries and Mathematical modeling

In this chapter, we establish the foundation of our study by outlining the mathematical models and reviewing fundamental concepts essential for further exploration. Initially, we define fluid mechanics and explore the concept and various types of fluids. Then we transition to introducing different mathematical models, starting with the SWM and extending to the SV-S system and its regularized type. We also discuss the transport equation and Boltzmann-type kinetic equations. Additionally, we provide background materials, including traveling wave solutions and fixed point theorems.

1.1 Fluid mechanics

1.1.1 What is the fluid mechanics

Fluid mechanics explores the behavior of fluids, both stationary and in motion, and is divided into two primary branches. Fluid statics examines fluids at rest, while fluid dynamics focuses on fluids in motion, including fields such as hydrodynamics.

Furthermore, fluid mechanics encompasses the study of the interaction between solids and fluids. This field has wide-ranging applications in various areas, such as aerodynamics, plasma studies, geophysics and hydraulics.

Fluid mechanics is important because it provides a well-developed mathematical theory that can be applied to various fields, particularly industries. This highlights its significance in multiple disciplines, especially in industrial sectors.

1.1.2 Concept of fluids

We differentiate between a solid and a fluid by [2] and [49]:

A fluid: **which is neither solid nor thick, which flows easily.**.

A solid is **something that has consistency but is not liquid.**.

From a microscopic point of view, a fluid is a body whose molecules slide easily past each other (liquid) or move freely relative to each other (gas).

A fluid is a body that is deformable under the action of very weak forces, and even if the deformation is large, this does not cause a loss of cohesion between its molecules. Fluid mechanics is interested in the deformations of fluids.

Liquid: **any body that flows or tends to flow.**

A liquid is characterized by its flow capacity and therefore has no shape of its own; it takes the shape of the container that contains it but has its own volume.

1.1.3 Types of Fluids

Fluids can be classified into various types, as outlined by [2] and [57]:

- **Ideal fluid:** This type of fluid is characterized by the absence of viscosity and incompressibility. However, ideal fluids do not exist in practical scenarios.
- **Real fluid:** Fluids with viscosity include compounds such as oil.

- **Newtonian fluid:** fluids that adhere to Newton's law of viscosity, such as water and most gases, have a constant viscosity regardless of the applied shear stress.
- **Non-Newtonian fluid:** like blood, do not have a constant viscosity.
- **Ideal plastic fluid:** is a form of fluid that behaves like a solid under specific conditions. For example clay.
- **Incompressible fluid:** Fluids whose density remains constant under the application of force such as water.
- **Compressible fluid:** This category includes fluids whose density varies with the application of force. For examples gas.

1.2 Mathematical models

1.2.1 Shallow water model

Usually, the SWM types of equations are applied when the horizontal flow length scale significantly exceeds the vertical fluid scale. Many authors have investigated this model for describing the hydrodynamics of rivers and lakes, see for example [12], [18], [23], [28] and [30].

In 2008, Mamadou et al. [10] derived a model with specified assumptions, written as follows:

- The depth and width are substantially smaller than the length of the river.
- The variations in water height are minimal.
- The domain's geometry remains fixed.
- The domain is assumed to have a rectangular shape.

- Energy and momentum fluxes are assessed for the whole river length.
- Only gravity force is considered, neglecting the influence of the Coriolis force.

Figure 1.1 shows the flow section presented as follows:

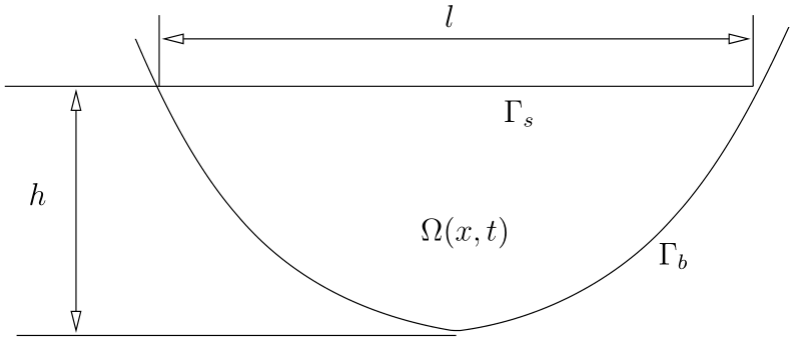

Figure 1.1: Flow section.

Let $\Omega = (0,T) \times \Gamma$, with $\Gamma = [0,L]$ such that L is positive strict, then the model proposed in [10] is written as follow:

$$\begin{cases} l\frac{\partial H}{\partial t} + \frac{\partial Q}{\partial x} = f_1, \\ \frac{\partial Q}{\partial t} - \nu\frac{\partial^2 Q}{\partial x^2} + \beta(H)\frac{\partial H}{\partial x} = f_2, \\ H(0,x) = H_0(x), \\ Q(0,x) = Q_0(x), \end{cases} \tag{1.1}$$

where the unknowns are H the height and q the discharge Q. The values l and ν are the width and viscosity respectively, $f1$ and f_2 are the external forces.

We studied the non-linear of this model theoretically and numerically by assuming β is non constant related to the flow height and the work cited in Lachache et al [33].

1.2.2 Saint-Venant system

The SV-S, which was developed by Saint-Venant in 1871 [46], is one of the shallow water models. The description of fluid flow in rivers is frequently done using this model and the foundation of the SV-S, are normally represented as follows:

Continuity equation:

$$\frac{\partial h}{\partial t} + \frac{\partial (hu)}{\partial x} = 0. \tag{1.2}$$

Momentum equation

$$\frac{\partial (hu)}{\partial t} + \frac{\partial}{\partial x}[hu^2 + \frac{1}{2}gh^2] + gh\frac{\partial z}{\partial x} = 0, \tag{1.3}$$

where the unknowns are h the height and u the velocity. The value g is the gravity and z stands for the bottom topography.

Figure 1.2 shows the flow section for the height with the bottom topography is not flat, as presented below:

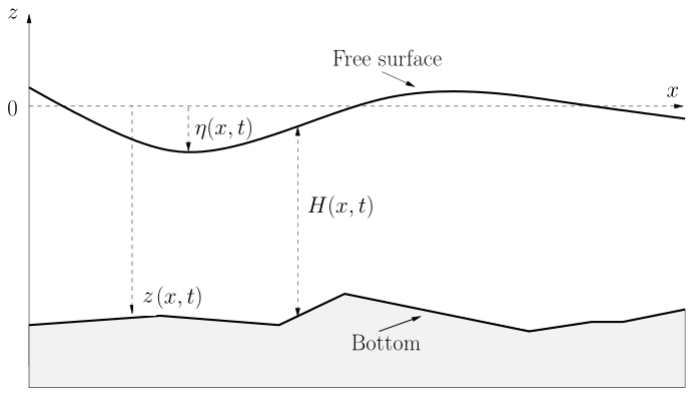

Figure 1.2: Presentation of the flow height.

Conservative forms of the SV-S

The SV-S variables are selected according to the following formulations

- **"velocity-water height" formulation:**

  The system in conservative form presented as follows:

$$\frac{\partial U}{\partial t} + \frac{\partial F(U)}{\partial x} + B(U) = 0, \tag{1.4}$$

$$U = \begin{pmatrix} h \\ hu \end{pmatrix}, F(U) = \begin{pmatrix} hu \\ hu^2 + \frac{gh^2}{2} \end{pmatrix}, B(U) = \begin{pmatrix} 0 \\ gh\frac{\partial z}{\partial x} \end{pmatrix}.$$

- **"flow-water height" formulation:**

  The system in conservative form presented as follows:

$$\frac{\partial U}{\partial t} + \frac{\partial F(U)}{\partial x} + B(U) = 0, \tag{1.5}$$

$$U = \begin{pmatrix} h \\ q \end{pmatrix}, F(U) = \begin{pmatrix} q \\ \frac{q^2}{h} + \frac{gh^2}{2} \end{pmatrix}, B(U) = \begin{pmatrix} 0 \\ gh\frac{\partial z}{\partial x} \end{pmatrix}.$$

Free surface

The free surface serves as the interface between air and water, typically maintaining a pressure equivalent to atmospheric pressure. Flows in natural (river) and artificial (irrigation, sanitation) channels are in most cases, free-surface flows. Free-surface flows are characterized by a water-to-air interface.

Figure 1.3 shows the behavior of the water flow, presented as follows:

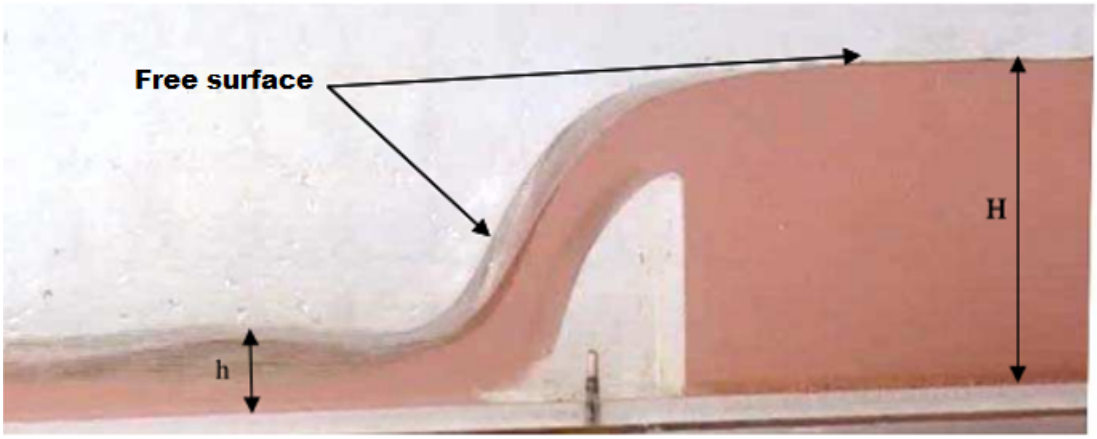

Figure 1.3: Free surface and flow height

1.2.3 Regularization of the SV-S

Several writers have expressed interest in models regularization, and the initial regularization was proposed by J. Leray [34] within the context of incompressible Navier-Stokes equations. His theoretical results demonstrated the well-posedness in regularized equations, serving as inspiration for many authors who have also proposed regularization techniques,see for example [14], [17] and [40].

The SV-S is a collection equations that govern the flow of shallow water in rivers. This system, which are based on mass and momentum conservation principles, has a large range of uses in hydraulic engineering and hydrology. However, this system is known to have certain mathematical and numerical instabilities, which is the classical SV-S in one dimension written as follows:

$$\begin{cases} \dfrac{\partial h}{\partial t} + \dfrac{\partial (hu)}{\partial x} = 0, \\ \dfrac{\partial (hu)}{\partial t} + \dfrac{\partial}{\partial x}[hu^2 + \frac{1}{2}gh^2] = 0. \end{cases} \tag{1.6}$$

Figure 1.4 shows the fluid domain of (1.6), presented as follows:

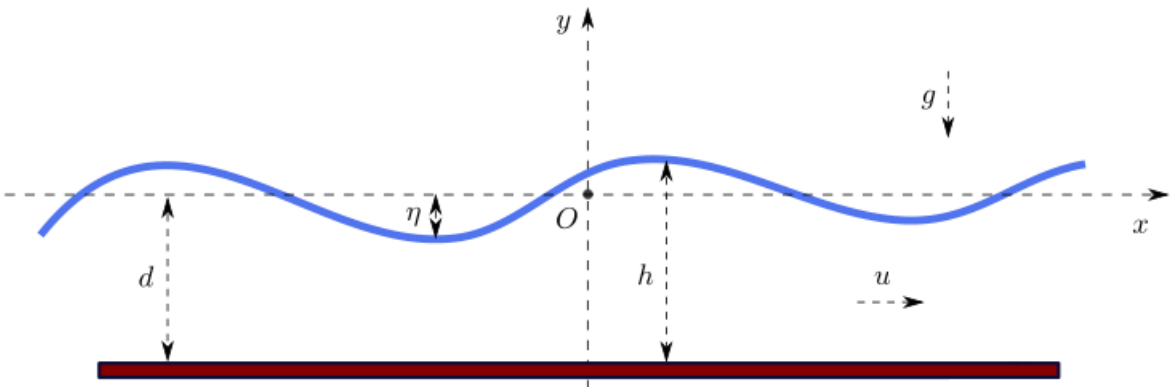

Figure 1.4: Flow section when the bottom topography is flat.

Ad a results, many authors are interested in the regularized type of this system, see for example [27]. Regularization techniques aim to alleviate these instabilities and improve the accuracy and stability of numerical simulations of shallow water flow. Several approaches have been devised to regularize the equations, with the goal of preventing discontinuous shocks.

In a recent work, [20] suggests a regularization of the nonlinear SV-S for flat bottoms. This system explain the propagation of lengthy gravity waves in two directions. They showed that the regularized of this system can be obtained from the Lagrangian density, which is represented as follows:

$$\ell = \frac{1}{2}hu^2 - \frac{1}{2}gh^2 + (h_t + [hu]_x)\phi + \frac{1}{2}\epsilon h^2(hu_x^2 - g_x^2),$$

where $\epsilon \geq 0$ is a regularisation parameter, and the resulting equations are

$$\begin{cases} h_t + [hu]_x = 0, \\ \partial_t[hu] + \partial_x[hu^2 + \frac{1}{2}gh^2 + \epsilon Rh^2] = 0, \end{cases} \tag{1.7}$$

where

$$R = h(u_x^2 - u_{xt} - uu_{xx}) - g(hh_{xx} + \frac{1}{2}h_2^x).$$

If $\epsilon = 0$, we can return to the classical Saint-Venant. Mathematical analysis of regularized Saint-Venant system is presented in [36] and [45].

1.2.4 Transport equation

The T-E, also known as the advection convection equation, illustrates the transport of a quantity by a fluid flow written as follows:

$$\frac{\partial p}{\partial t} + u\frac{\partial p}{\partial x} = D\frac{\partial^2 p}{\partial x^2}, \tag{1.8}$$

where p denotes the transported quantity, encompassing parameters like density, concentration,..., u represents the fluid's velocity and D stands for the diffusion coefficient.

this equation describes the physical phenomenon where a quantity is transferred inside a physical system, attributed to two principal mechanisms: advection and diffusion.

1. Advection refers to the phenomenon wherein a substance is conveyed by the collective motion of a fluid. An illustrative example is the transportation of smoke by wind currents. In mathematical terms, advection is manifested through spatial derivatives.

2. Diffusion denotes the mechanism through which a substance diffuses from regions of high concentration to those of lower concentration, driven by the stochastic motion of particles, such as molecular or Brownian motion. In mathematical representation, diffusion is characterized by second-order spatial derivatives.

The T-E finds extensive application across disciplines such as fluid mechanics and chemical engineering, facilitating the comprehension and prediction of substance transport and dis-

persion within a flowing medium. It holds significant importance in modeling phenomena including pollutant dispersion, heat transfer, and the conveyance of chemical species within industrial and environmental systems.

1.2.5 Boltzmann-type kinetic equations

Boltzmann-type kinetic equations are a powerful tool for describing the behavior of gas particles in terms of probability distributions. They provide a fundamental framework for understanding the macroscopic properties of gases, plasmas and other systems.
The fundamental form is expressed as:

$$\frac{\partial f}{\partial t} + \xi \cdot \nabla_{\xi} + F \cdot \nabla_{\xi} f = \Omega(f),$$

where f is the distribution function, ξ is velocity vectors, F is the external force, and $\Omega(f)$ is the collision operator. This equation dictates the temporal development of particle distribution functions in phase space., encompassing both position and momentum, in response to phase space advection, external forces, and collisions.
Many researchers have been interested in this type of equation and useful for the kinetic method were introduced in [31] and [42] for the numerical processing of Euler's equations, after that many authors use this idea see for example [4], [5], [23] and [44].

Gibbs equilibrium

The definition of Gibbs equilibrium, also known as a microscopic density of particles of a specific form and named after the physicist Josiah Willard Gibbs [24], denotes a state in which the properties of a physical system, such as temperature, pressure, remain constant over time, see for example the work of Sethna cited in [47].

One of the expression of Gibbs equilibrium is as follows:

$$M(t,x,\xi) = \frac{h(t,x)}{c(t,x)}\chi\left(\frac{\xi - U(x)}{c(t,x)}\right),$$

Where ξ designates an additional variable homogeneous at a speed, and c the speed of the information. The function χ is an even probability density whose second moment is equal to 1. This definition establishes a relationship between the kinetic and macroscopic levels of the Boltzmann type kinetic equation written as follows

$$\partial_t M + \xi \partial_\xi M = Q(t, x\xi),$$

where Q represent the collision term such that

$$\int_R \begin{pmatrix} 1 \\ \xi \end{pmatrix} Q_1 d\xi = 0. \tag{1.9}$$

We introduce in the chapter fourth a kinetic approach to our system and present theoretical results on its well posedness based on the Boltzmann type kinetic equation.

1.3 Background materials

Definition 1.3.1 *([6], [13] and [51].)*
A Banach space is defined as a complete normed vector space. Specifically, consider a vector space E equipped with a norm $(||\bullet||)$. The pair $(E, ||\bullet||)$ is termed a Banach space if E is complete under the metric induced by the norm $||\bullet||$. In other words, every Cauchy sequence in E has a limit within E, ensuring the space's completeness.

Definition 1.3.2 *([32]) The space $C(E)$ is the set of all bounded and continuous functions*

in space E, equipped with a suitable norm. For a function $f \in C(E)$ such that:

$$||f||_\infty = sup|f(x)| : x \in E,$$

where sup denotes the supremum of the set of absolute values of $f(x)$ for all $x \in E$.

1.3.1 Traveling wave Solutions

Traveling wave solutions are special solutions to differential equations that represent wave-like behavior moving across a material at a fixed velocity without changing its shape. The significance of the traveling wave solution lies in its application, as it enables the modeling of dynamics in numerous physics problems, chemistry, engineering and many topics from theoretical aspects to computational methods and applications in different scientific fields. see for example [8], [21], [26], [35], [48] and [55].

The Traveling wave form for PDEs written as follows

$$u(x,t) = \psi(\eta), \tag{1.10}$$

where, $\eta = x - ct$ and c is strictly positive constant.

We utilize the concept of traveling wave solutions to establish the well-posedness of our models.

1.3.2 Fixed Point Theorems

In the remainder of this part, we introduce certain definitions and theorems related to the Ascoli-Arzela theorem and other theorems necessary for this study.

Definition 1.3.3 ***(Compact Set)****[51]*

A set E in a metric space is said to be compact if every open set of E has a finite subset. In

other words, for every open set $f_n \in E$, there exists a finite subset $f_1, f_2, f_3, ..., f_n$ that also covers E

Definition 1.3.4 *(Equicontinuous [7])*

Let E be a Banach space. A familly of functions f_n in E is called equicontinuous if

$$\forall \psi > 0, \forall n_1, n_2 \in E, \forall A \in P || n_1 - n_2 || < \delta \Rightarrow ||A(n_1) - A(n_2)|| < \psi$$

Theorem 1.3.5 *(Ascoli-Arzelà [25])*

Let E be a compact space and f_n be a sequence of continuous functions such that $f_n \in C(E)$. If $A(P)$ is an equicontinuous and bounded subset of $C(E)$ (i.e., there exists an $M > 0$ such that $|f_n| \leq M$ for all $x \in E$), then A is relatively compact.

In addition to the Ascoli-Arzela theorem, we introduce the definitions and theorems related to these fixed point theorems.

Definition 1.3.6 *(Contraction principal [25])*

Let E be any space and $A : E \longrightarrow E$ is called a contraction mapping (or a subset of E, into E), there exists $k \in (0, 1)$ such that

$$\forall \phi, \phi_1 \in E, \quad ||A\phi - A\phi_1|| \leq k||\phi - \phi_1||$$

Theorem 1.3.7 *(Banach's fixed point [25])*

Let A be a non-empty closed subset of a Banach space E, then every contraction mapping A of E has a unique fixed point. There exists a unique point $x^* \in E$ such that $A(x^*) = x^*$

Theorem 1.3.8 *(Schauder's fixed point [25])*

Let E be a Banach space, and K be a closed, convex and nonempty subset of E. Let $A : K \longrightarrow K$ be a continuous mapping. Then A has at least one fixed point x^* in K such that $A(x^*) = x^*$.

Chapter 2

Theoretical and numerical results for a shallow water model

In this chapter, we establish the well-posedness of (1.1), when β is not constant related to the flow height H.

This chapter is organized as follows. We start by establishing our model. Next, we utilize the traveling wave solution to prove the well-posedness of this model and provide an explicit solutions based on the traveling wave solutions. Following this, we present numerical discretizations using finite difference method. Numerical results along with corresponding comments, we finish with conclusion remark.

2.1 Proposed model

Let a and b, be positive constants, and we assume β of (1.1) is a continuous function such that

$$\beta(H) = a + 2bH, \tag{2.1}$$

where $a = lU^2 + \frac{p_a l}{U^2}$ and $b = \frac{gl^2}{2U^2}$, with g is the gravity, U the characteristic velocity and p_a the atmospheric pressure.

Let $\Omega = (0, T) \times \Gamma$, with $\Gamma = [0, L]$ such that L is positive strict, then the proposed model is one dimension presented as follows

$$\begin{cases} l\frac{\partial H}{\partial t} + \frac{\partial Q}{\partial x} = f_1, \\ \frac{\partial Q}{\partial t} - \nu\frac{\partial^2 Q}{\partial x^2} + a\frac{\partial H}{\partial x} + 2bH\frac{\partial H}{\partial x} = f_2, \\ H(0, x) = H_0, \\ Q(0, x) = Q_0, \end{cases} \tag{2.2}$$

where the unknowns are the flow height H and the discharge Q. The values l and ν are the width and viscosity respectively and external forces are $f1$ and f_2.

Let $K \in \mathbb{R}^*$, and we already know that H must be limited, then $\forall (t, x) \in \Omega$

$$\sup_{(t,x)\in\Omega} |H| \leq K, \tag{2.3}$$

the use of this inequality help us to determine the well-posdness of (2.2).

Let λ be a strictly positive constant, and $\eta = x - ct$ such that $\eta \in [0, \lambda]$ and c is strictly positive constant denotes the traveling wave velocity. We assume that

$$\begin{cases} h(x, t) = \varrho(\eta), \\ q(x, t) = \sigma(\eta), \end{cases} \tag{2.4}$$

Using (2.3) in (2.4), yields

$$\sup_{(t,x)\in\Omega} |\varrho| \leq M. \tag{2.5}$$

By substituting (2.4) in (2.2), we obtain

$$\begin{cases} -lc\varrho'(\eta) + \sigma'(\eta) = f_1, \\ -c\sigma'(\eta) - \nu\sigma''(\eta) + (a + 2b\varrho(\eta))\varrho'(\eta) = f_2, \\ \varrho(\eta)_{t=0} = \varrho_0, \\ \sigma(\eta)_{t=0} = \sigma_0. \end{cases} \tag{2.6}$$

By integrating the second equation of (2.6), we obtain

$$\begin{cases} \varrho'(\eta) = \frac{1}{lc}(\sigma'(\eta) - f_1), \\ \sigma'(\eta) = \sigma_1 + \frac{1}{\nu}\int_0^\eta \left(a\varrho'(\eta) + 2b\varrho(\eta)\varrho'(\eta) - c\sigma'(\eta) - f_2\right) d\eta, \quad \sigma_1 = \sigma'(0), \\ \varrho(\eta)_{t=0} = \varrho_0, \\ \sigma(\eta)_{t=0} = \sigma_0. \end{cases} \tag{2.7}$$

By using fixed-point theorems, we develop the essential parameters for finding at least one solution and determining its uniqueness.

2.2 Main Results

Starting with the fundamental and crucial definitions. Let $C([0,\lambda],\mathbb{R})$ a Banach space of continuous functions from $[0,\lambda] \longrightarrow \mathbb{R}$, such that

$$\|\varrho\|_\infty = \sup_{\eta\in[0,\lambda]} |\varrho|. \tag{2.8}$$

Let $u = (\varrho, \sigma)$ be solutions of of (2.7), this implies

$$\begin{cases} \varrho'(\eta) = \kappa_1(\eta, u(\eta)), \\ \sigma'(\eta) = \kappa_2(\eta, u(\eta)), \end{cases} \tag{2.9}$$

where $\kappa_{1\leq i\leq 2}(\eta, u(\eta))$ is the right hand side of (2.7).

By applying fixed-point theory, we demonstrate the existence of at least one solution of (2.7).

Let $u = (\varrho, \sigma) \in E$, such that $E = [C([0, \lambda], \mathbb{R}_+]^2$ with the norm

$$\|u\|_E = \|\varrho\|_\infty + \|\sigma\|_\infty. \tag{2.10}$$

let $\kappa = (\kappa_1, \kappa_2)$ such that

$$\begin{cases} \kappa_1(\eta, u(\eta)) = \frac{1}{lc}(\sigma'(\eta) - f_1), \\ \kappa_2(\eta, u(\eta)) = \sigma_1 + \dfrac{1}{\nu}\int_0^\eta \left(a\varrho'(\eta) + 2b\varrho\varrho'(\eta) - c\sigma'(\eta) - f_2\right) d\eta, \end{cases} \tag{2.11}$$

Clearly, $\kappa \in ([0, \lambda] \times E)^2$ is continuous.

Applying the integral to both sides of (2.11), yields:

$$\begin{cases} \varrho(\eta) = \varrho(0) + \int_0^\eta \kappa_1(\xi, u(\xi))d\xi, \\ \sigma(\eta) = \sigma(0) + \int_0^\eta \kappa_2(\xi, u(\xi))d\xi. \end{cases} \tag{2.12}$$

By choosing $u_0 = (u_1, u_2) = (\varrho(0), \sigma(0))$, we obtain

$$u(\eta) = u_0 + \int_0^\eta \kappa(\xi, u(\xi))d\xi.$$

Below, we present the main results:

Theorem 2.2.1 *(**Existence**) let a, b, c, K, l, λ, ν and $\mu \in \mathbb{R}_+$ with*

$$\mu = max\{\frac{1}{lc}, \frac{\lambda}{\nu}(a + 2bK + c)\},$$

if

$$\mu < 1. \tag{2.13}$$

Then, there is at least one solution to (2.7) *on* $[0, \lambda]$.

Proof. We transform (2.7) into a fixed-point problem written in this form $Fu(\eta) = u(\eta)$, such that:

$$Fu(\eta) = (F_1u(\eta), F_2u(\eta)),$$

and

$$F_iu(\eta) = u_0 + \int_0^\eta \kappa_i(\xi, u(\xi))d\xi, \quad i = 1, 2. \tag{2.14}$$

We determine that if $u \in E$, then $(F_iu)_{1\leq i\leq 2}$ is a continuous operator. Thus, $Fu \in E$ with

$$\|Fu\|_E = \sum_{i=1}^{2} \|F_iu\|_\infty.$$

Next, we establish that F meets the requirements of Schauder's fixed-point theorem using the following steps:

- **Step 1:** F is a continuous operator.

  Let $(u_n)_{n\in N} = (\varrho_n, \sigma_n)$ be two positive sequences such that $\lim\limits_{x\to+\infty} u_n = u$ in E, we have $\lim\limits_{x\to+\infty} \varrho_n = \varrho$ and $\lim\limits_{x\to+\infty} \sigma_n = \sigma$ in E.

  Then, we have

$$
\begin{aligned}
|F_1u_n(\eta) - F_1u(\eta)| &= |\int_0^\eta \kappa_1(\xi, u_n(\xi))d\xi - \int_0^\eta \kappa_1(\xi, u(\xi))d\xi|, \\
&= |\int_0^\eta \frac{1}{lc}(\sigma_n'(\xi) - f_1)d\xi - \int_0^\eta \frac{1}{lc}(\sigma'(\xi) - f_1)d\xi|, \\
&= |\frac{1}{lc}(\sigma_n(\eta) - \sigma_n(0) - \eta f_1) - \frac{1}{lc}(\sigma(\eta) - \sigma(0) - \eta f_1)|, \quad (2.15) \\
&= \frac{1}{lc}|(\sigma_n(\eta) - \sigma(\eta))|, \\
&\leq (\frac{1}{lc})\|u_n - u\|_E.
\end{aligned}
$$

Similarly, we obtain

$$
\begin{aligned}
|F_2u_n(\eta) - F_2u(\eta)| &= |\int_0^\eta \kappa_2(\xi, u_n(\xi))d\xi - \int_0^\eta \kappa_2(\xi, u(\xi))d\xi|, \\
&= |\int_0^\eta \left(\sigma_1 + \frac{1}{\nu}\int_0^\eta a\varrho_n' + 2b\varrho_n\varrho_n' - c\sigma_n' - f_2 d\xi\right) d\xi, \\
&- \int_0^\eta \left(\sigma_1 + \frac{1}{\nu}\int_0^\eta a\varrho' + 2b\varrho\varrho' - c\sigma' - f_2 d\xi\right) d\xi|, \\
&= |\frac{1}{\nu}\int_0^\eta (a\varrho_n + b\varrho_n^2 - c\sigma_n)\, d\xi - \frac{1}{\nu}\int_0^\eta (a\varrho + b\varrho^2 - c\sigma)\, d\xi|, \\
&\leq \frac{1}{\nu}\left(\int_0^\eta a|\varrho_n - \varrho|d\xi + b\int_0^\eta |\varrho_n^2 - \varrho^2|d\xi + c\int_0^\eta |\sigma_n - \sigma_u|d\xi\right), \quad (2.16) \\
&\leq \frac{1}{\nu}\{\int_0^\eta a|\varrho_n - \varrho|d\xi + b\int_0^\eta |\varrho_n(\varrho_n - \varrho) + \varrho_u(\varrho_n - \varrho)|d\xi \\
&+ c\int_0^\eta |\sigma_n - \sigma|d\xi\}, \\
\text{by using} \quad (2.5) \qquad &\leq \frac{1}{\nu}\{\int_0^\eta a|\varrho_n - \varrho|d\xi + 2bK\int_0^\eta |\varrho_n - \varrho_u|d\xi + c\int_0^\eta |\sigma_n - \sigma|\}, \\
&\leq \frac{\lambda}{\nu}(a + 2bK + c)\|u_n - u\|_E,
\end{aligned}
$$

if we consider $\mu = max\{\frac{1}{lc}, \frac{\lambda}{\nu}(a + 2bK + c)\}$, then we have

$$|F_iu_n(\eta) - F_iu(\eta)| \leq \mu\|u_n - u\|_E,\ \mu > 0,\ i = 1, 2.$$

Since $u_n \longrightarrow u$ in E, A is continuous.

- **Step 2:** $A(E_j) \subset E_j$.

Let j be a real positive number such that

$$j \geq \frac{2}{1-2\mu} u_i.$$

The subset E_j defined as follows:

$$E_j = \{u \in E : \|u\|_E \leq j\}.$$

Clearly E_j represents a closed, bounded and convex subset of E.

Let $A : E_j \to E$ be an integral operator given by (2.14), thus $F(E_j) \subset E_j$, we get

$$\begin{aligned} |F_1 u(\eta)| &\leq u_1 + \frac{1}{lc} j, \\ |F_2 u(\eta)| &\leq u_2 + \frac{1}{\nu}(\frac{\lambda}{\nu}(a + 2bK + c)j. \end{aligned} \tag{2.17}$$

Hence, in each case, we have

$$\begin{aligned} |F_i u(\eta)| &\leq u_i + \mu j, \\ &\leq \frac{1-2\mu}{2} r + \mu j, \\ &\leq \frac{1}{2} j, \quad i = 1, 2, \end{aligned} \tag{2.18}$$

or $(\|F_i u\|_\infty)_{1 \leq i \leq 2} \leq \dfrac{j}{2}$, then

$$\|Fu\|_E = \sum_{i=1}^{2} \|F_i u\|_\infty \leq j.$$

then, $F(E_j) \subset E_j$ holds.

- **Step 3:** $F(E_j)$ is relatively compact.

Let $\eta_1, \eta_2 \in [0, \lambda]$, such that $\eta_1 < \eta_2$ and $u \in E_j$, then we have

$$\begin{aligned} |F_1u(\eta_1) - F_1u(\eta_2)| &= |\int_0^{\eta_2} \kappa_1(\xi, u(\xi))d\xi - \int_0^{\eta_1} \kappa_1(\xi, u(\xi))d\xi|, \\ &= |\int_0^{\eta_2} \frac{1}{lc}(\sigma'(\xi) - f_1)d\xi - \int_0^{\eta_1} \frac{1}{lc}(\sigma'(\xi) - f_1)|d\xi, \\ &\leq |\frac{1}{lc}\left(\sigma(\eta_2) - \eta_2 f_1 - \sigma(\eta_1) + \eta_1 f_1\right)|, \\ &\leq |\frac{1}{lc}\left(\sigma(\eta_2) - \sigma(\eta_1) - (\eta_2 - \eta_1)f_1\right)|, \\ &\leq |\frac{1}{lc}(|\sigma(\eta_2) - \sigma(\eta_1)| + |(\eta_2 - \eta_1)f_1|), \end{aligned} \tag{2.19}$$

we already know that σ is continuous, this implies $\sigma(\eta_1) \to \sigma(\eta_2)$.

It follows from $\eta_1 \to \eta_2$, that the inequality (2.19) tends to zero, which means

$$|F_1u(\eta_1) - F_1u(\eta_2)| \leq 0. \tag{2.20}$$

Similarly, we have

$$\begin{aligned} |F_2u(\eta_1) - F_2u(\eta_2)| &= |\int_0^{\eta_2} \kappa_2(\xi, u(\xi))d\xi - \int_0^{\eta_1} \kappa_2(\xi, v(\xi))d\xi|, \\ &= |\int_0^{\eta_2}(\sigma_1(\xi) + \frac{1}{\nu}\int_0^{\eta_2} a\varrho'(\xi) + 2b\varrho\varrho'(\xi) - c\sigma'(\xi) - f_2)d\xi \\ &- \int_0^{\eta_1}(\sigma_1(\xi) + \frac{1}{\nu}\int_0^{\eta_1} a\varrho'(\xi) + 2b\varrho(\xi)\varrho'(\xi) - c\sigma'(\xi) - f_2)d\xi|, \\ &= |(\eta_2 - \eta_1)\sigma_1 + \frac{1}{\nu}(a(\varrho(\eta_2) - \varrho(\eta_1)) + b(\varrho^2(\eta_2) - \varrho^2(\eta_1)), \\ &- c(\sigma(\eta_2) - \sigma(\eta_1)) - (\eta_2 - \eta_1)f_2)|. \end{aligned} \tag{2.21}$$

σ and ϱ are continuous, i.e. $\sigma(\eta_1) \to \sigma(\eta_2)$, $\varrho(\eta_1) \to \varrho(\eta_2)$.

It follows from $\eta_1 \to \eta_2$, that inequality (2.21) tends to zero.

$$|F_2u(\eta_1) - F_2u(\eta_2)| \leq 0. \tag{2.22}$$

Then from (2.20) and (2.22) we obtain

$$|F_i u(\eta_1) - F_i u(\eta_2)| \leq 0, \quad i = 1, 2.$$

Steps 1-3 and the Ascoli-Arzela theorem confirm the continuity and compactness of $F : E_j \to E_j$, implying that it satisfies Schauder's fixed point theorem [25]. Thus, F has a fixed-point solution of (2.7) on $[0, \lambda]$.

In Theorem 2.2.1, we established that (2.7) has at least one possible solution.
If Theorem 2.2.1 holds for all $(x, t) \in \Omega$, there is at least one solution of (2.2) under the traveling wave form (2.4).

Theorem 2.2.2 *(**Uniqueness**) let a, b, c, K, l, λ, ν and $\mu \in \mathbb{R}_+$ with*

$$\mu = max\{\frac{1}{lc}, \frac{\lambda}{\nu}(a + 2bK + c)\},$$

if

$$\mu < 1, \tag{2.23}$$

then, (2.7) *admits a unique solution on* $[0, \lambda]$.

Proof. In Theorem 2.2.1., We have previously transformed (2.7) into a fixed-point problem. Assume $u, v \in E$ and (2.7). This indicates the following:

$$\begin{aligned} |F_1 u(\eta) - F_1 v(\eta)| &\leq \tfrac{1}{lc}\|u - v\|_E, \\ |F_2 u(\eta) - F_2 v(\eta)| &\leq \frac{\lambda}{\nu}(a + 2bK + c)\|u - v\|_E. \end{aligned} \tag{2.24}$$

We assume that $\mu = max\{\frac{1}{lc}, \frac{\lambda}{\nu}(a + 2bK + c)\}$, this implies

$$\|F_i u - F_i v\|_\infty \leq \mu \|u - v\|_E.$$

Similarly, we can find that:

$$\|Fu - Fv\|_E \leq \mu \|u - v\|_E. \tag{2.25}$$

Theorem 2.2.1 and (2.25) indicate that F is a contraction. According to Banach's contraction principle (see [25]), F has a single fixed point, which is the unique solution of (2.7). Based on Theorem 2.2.2, there is a unique solution of (2.2) if (2.23) holds.

2.2.1 Explicit Solution

We assume $(f_1, f_2) = 0$, system (2.6) written as follows

$$\begin{cases} -lc\varrho'(\eta) + \sigma'(\eta) = 0, \\ -c\sigma'(\eta) - \nu\sigma''(\eta) + (a + 2b\varrho(\eta))\varrho'(\eta) = 0, \\ \varrho(\eta)_{t=0} = \varrho_0, \\ \sigma(\eta)_{t=0} = \sigma_0. \end{cases} \tag{2.26}$$

This implies

$$\begin{cases} \varrho'(\eta) = \frac{\sigma'(\eta)}{lc}, \\ \sigma'(\eta) = \frac{-\nu\sigma''(\eta) + (a+2b\varrho(\eta))\varrho'(\eta)}{c}. \end{cases} \tag{2.27}$$

By substituting the first equation of (2.27) in the second one, we obtain

$$\sigma'(\eta) = \frac{-\nu\sigma''(\eta)}{c} + \frac{(a + 2b\sigma'(\eta))\sigma'(\eta)}{lc^2}. \tag{2.28}$$

By integrating (2.28), we obtain

$$\sigma(\eta) = \frac{-\nu\sigma(\eta)'}{c} + \frac{a\sigma(\eta)}{lc^2} + \frac{b\sigma^2(\eta)}{lc^2} + C_0, \tag{2.29}$$

such that $C_0 = \sigma(\eta)_0 - \nu\sigma(\eta)'_0 + \frac{a\nu\sigma(\eta)}{lc^2}$. This implies

$$\sigma'(\eta) = (\frac{-c}{\nu} + \frac{a}{lc\nu})\sigma(\eta) + \frac{b}{lc\nu}\sigma^2(\eta) + C_0. \tag{2.30}$$

If we assume that $a = lc(\nu + c)$ and $b = lc\nu$, (2.30) becomes

$$\sigma'(\eta) = \sigma(\eta) + \sigma^2(\eta) + C_0. \tag{2.31}$$

We can find easily the solution of (2.31) written as follows

$$\sigma(\eta) = \frac{\alpha - \kappa\beta e^{(\alpha-\beta)\eta}}{1 - \kappa\beta e^{(\alpha-\beta)\eta}}, \tag{2.32}$$

where $\alpha = \frac{-1+\sqrt{1-4C_0}}{2}$ and $\beta = \frac{-1-\sqrt{1-4C_0}}{2}$ and $\kappa = e^{(\alpha-\beta)C_1}$. This implies that

$$\varrho(\eta) = \frac{\alpha - \kappa\beta e^{(\alpha-\beta)\eta}}{lc(1 - \kappa\beta e^{(\alpha-\beta)\eta})}. \tag{2.33}$$

From (2.32) and (2.33), we get

$$H(x,t) = \frac{\alpha - \kappa\beta e^{(\alpha-\beta)(x-ct)}}{lc(1 - \kappa\beta e^{(\alpha-\beta)(x-ct)})}, \tag{2.34}$$

$$Q(x,t) = \frac{\alpha - \kappa\beta e^{(\alpha-\beta)(x-ct)}}{1 - \kappa\beta e^{(\alpha-\beta)(x-ct)}}. \tag{2.35}$$

Figures $2.1 - 2.4$ show the variation of an explicit solutions for the height H and discharge Q, presented as follows:

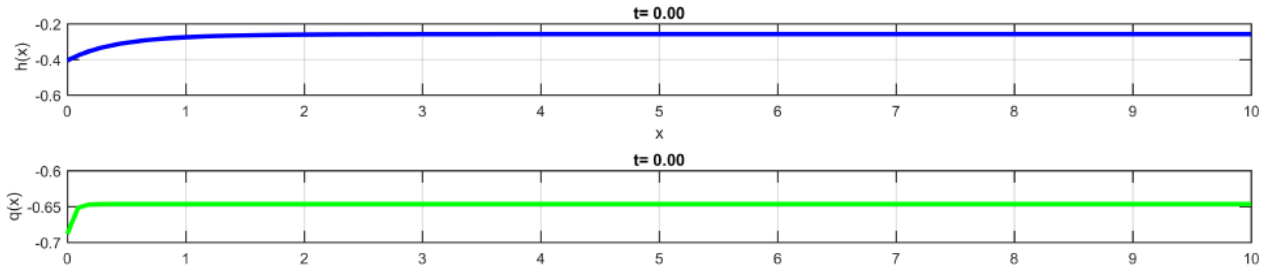

Figure 2.1: Initial solutions of (2.2) and (1.1) for the height H and the discharge Q.

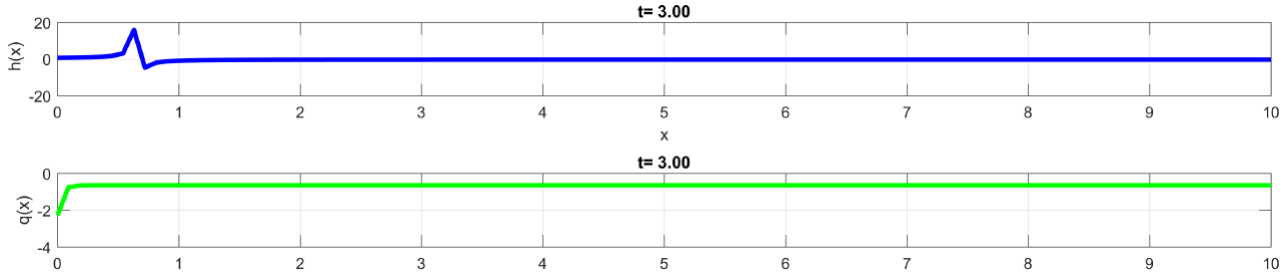

Figure 2.2: Solutions of (2.2) and (1.1) for the height H and the discharge Q, at $t = 3$.

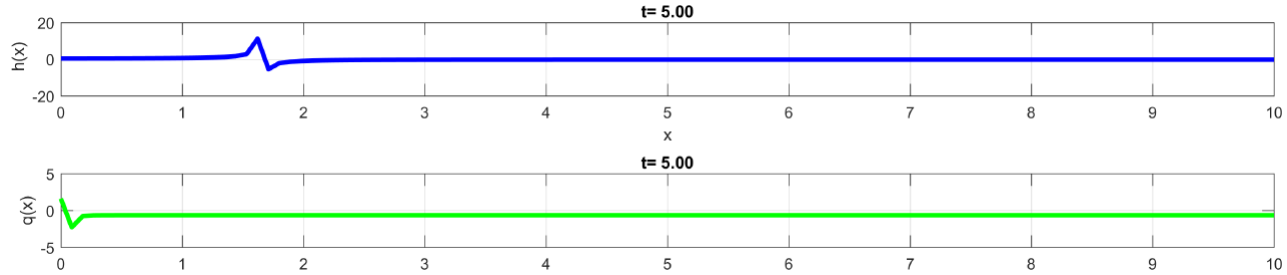

Figure 2.3: Solutions of (2.2) and (1.1) for the height H and the discharge Q, at $t = 5$.

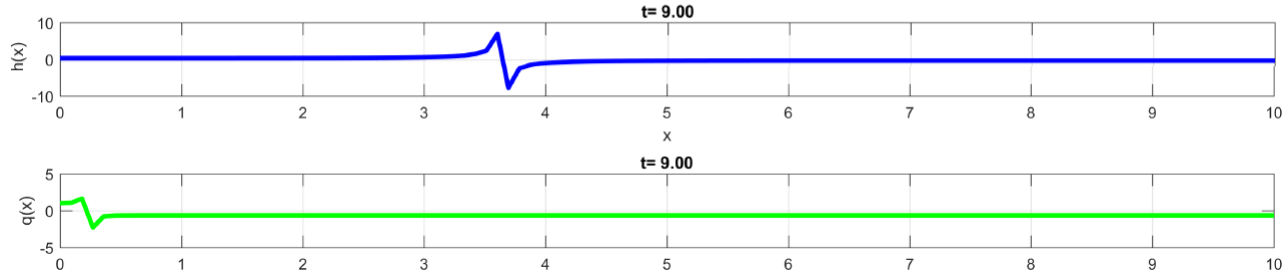

Figure 2.4: Solutions of (2.2) and (1.1) for the height H and the discharge Q, at $t = 9$.

Comment

The parameters of (2.34) and (2.35) are chosen adaptively and presented as follows: the traveling wave velocity $c = 12$, the width $l = 5$, the values $C_0 = 1/8$ and $C_1 = 1$.
The obtained results from these solutions demonstrate the variations in the low height H and flow discharge Q, and we observe a decreasing solution behavior for each one over time.

2.3 Numerical Approximation

In this part, we discretize (2.2) with $(f_1, f_2) = 0$ and establish a stability condition for the proposed numerical method.

2.3.1 Finite difference approximation

We use an explicit finite difference approach to discretize (2.2). The temporal and spatial derivatives are defined as follows:

$$\frac{\partial H}{\partial t} = \frac{H_i^{n+1} - H_i^n}{\Delta t}, \tag{2.36}$$

$$\frac{\partial H}{\partial x} = \frac{H_{i+1}^n - H_{i-1}^n}{2\Delta x}. \tag{2.37}$$

Thus, we get

$$l\frac{H_i^{n+1} - H_i^n}{\Delta t} + \frac{Q_{i+1}^n - Q_{i-1}^n}{2\Delta x} = 0, \tag{2.38}$$

$$\begin{aligned}\frac{Q_i^{n+1}-Q_i^n}{\Delta t} &= \nu\left(\frac{Q_{i+1}^n-2Q_i^n+Q_{i-1}^n}{(\Delta x)^2}\right)-a\left(\frac{H_{i+1}^n-H_{i-1}^n}{2\Delta x}\right)\\ &- bH_i^n\left(\frac{H_{i+1}^n-H_{i-1}^n}{2\Delta x}\right),\end{aligned} \tag{2.39}$$

then, we obtain $H_i^{n+1}$and Q_i^{n+1}:

$$H_i^{n+1}=H_i^n-\frac{\Delta t}{l}\left(\frac{Q_{i+1}^n-Q_{i-1}^n}{2\Delta x}\right). \tag{2.40}$$

$$\begin{aligned}Q_i^{n+1} &= Q_i^n-\Delta t\left(-\nu\left(\frac{Q_{i+1}^n-2Q_i^n+Q_{i-1}^n}{(\Delta x)^2}\right)-a\left(\frac{H_{i+1}^n-H_{i-1}^n}{2\Delta x}\right)\right)\\ &- \Delta t b H_i^n\left(\frac{H_{i+1}^n-H_{i-1}^n}{2\Delta x}\right).\end{aligned} \tag{2.41}$$

2.3.2 Stability analysis

We establish a result concerning the numerical stability of (2.40)-(2.41) and present its numerical implementation.

Proposition 2.3.1 *Numerical scheme* (2.40) *is stable under the following conditions:*

$$\Delta t\leq 2l\Delta x. \tag{2.42}$$

Proof. To demonstrate this result, we employ Fourier analysis: We express the solution in the form (see [11] and [41]):

$$H_j^n=\lambda^n e^{i\pi\kappa j}, \tag{2.43}$$

$$Q_j^n=\lambda^n e^{i\pi\kappa j}, \tag{2.44}$$

where κ an integer in (2.40), this implies

$$\lambda = \lambda^n e^{i\pi\kappa j} - \frac{\Delta t}{l}\left(\frac{\lambda^n e^{i\pi\kappa(j+1)} - \lambda^n e^{i\pi\kappa(j-1)}}{2\Delta x}\right). \tag{2.45}$$

If we divide by $\lambda^n e^{\pi\kappa j}$ in (2.45), we get

$$\lambda = 1 - \frac{\Delta t}{l}\left(\frac{cos(\pi\kappa)}{\Delta x}\right). \tag{2.46}$$

If $|\lambda| \leq 1$, numerical scheme (2.40) is stable, and thus we obtain

$$|1 - \frac{\Delta t}{l}\left(\frac{cos(\pi\kappa)}{\Delta x}\right)| \leq 1. \tag{2.47}$$

This implies

$$|1 - \frac{\Delta t}{l\Delta x}| \leq 1, \tag{2.48}$$

then

$$\Delta t \leq 2l\Delta x. \tag{2.49}$$

Proposition 2.3.2 *numerical scheme* (2.41) *is stable under the following conditions:*

$$\Delta t \leq \frac{2(\Delta x)^2}{4\nu + a\Delta x + bH_m\Delta x}, \tag{2.50}$$

with $H_m = max(H_j^n)$.

Proof. Similarly, we can prove it by using the same technique as in 2.3.1., and obtain

$$\lambda = 1 - \Delta t\left(-\nu\frac{2cos(\pi\kappa) - 2}{(\Delta x)^2} + a\frac{cos(\pi\kappa)}{\Delta x}\right) - \Delta t b H_m\left(\frac{cos(\pi\kappa)}{\Delta x}\right). \tag{2.51}$$

By using this formula $cos(\pi\kappa) - 1 = -2sin^2\left(\frac{\pi\kappa}{2}\right)$ in (2.51), we obtain

$$\lambda = 1 - \Delta t \left(\nu \frac{4sin^2\left(\frac{\pi\kappa}{2}\right)}{(\Delta x)^2} + a\frac{cos(\pi\kappa)}{\Delta x} \right) - \Delta t b H_m \left(\frac{cos(\pi\kappa)}{\Delta x} \right). \tag{2.52}$$

If $|\lambda| \leq 1$, numerical scheme (2.41) is stable, and thus we obtain

$$|1 - \Delta t \left(\nu \frac{4sin^2\left(\frac{\pi\kappa}{2}\right)}{(\Delta x)^2} + a\frac{cos(\pi\kappa)}{\Delta x} \right) - \Delta t b H_m \left(\frac{cos(\pi\kappa)}{\Delta x} \right)| \leq 1, \tag{2.53}$$

we have $sin^2\left(\frac{\pi\kappa}{2}\right) \leq 1$ and $cos(\pi\kappa) \leq 1$ which implies

$$|1 - \Delta t \left(\frac{4\nu}{(\Delta x)^2} + a\frac{1}{\Delta x} + bH_m\frac{1}{\Delta x} \right)| \leq 1, \tag{2.54}$$

then

$$0 \leq \Delta t \leq \frac{2(\Delta x)^2}{4\nu + a\Delta x + bH_m\Delta x}. \tag{2.55}$$

2.3.3 Numerical results and comments

Numerical results

To solve (2.40)-(2.41) numerically, we apply the algorithm presented as follows

Algorithm:

- Step 1 (Initialization): input the gravity g, length L and width l, viscosity ν, coefficients a and b, space step Δx, time step Δt, final time T and the starting solution for the height H_0 and discharge Q_0.
- Step 2: solve (2.40) for the height H.

- Step 3: solve (2.41) for the discharge Q.
- Step 4: Repeat steps 2 and 3 until T is reached.

Figures $2.1 - 2.3$ summarize the obtained results for the solutions of (1.1) and (2.2), demonstrating the change in the height and discharge at different times and locations.
The discretization parameters written as follows: $\Delta x = 0.3$ and Δt according to the CFL conditions (2.42) and (2.50), length $L = 1$, width $l = 1/2$, viscosity $\nu = 5 * 10^{-3}$, coefficient $b = l^2 \cdot g \cdot T^2/(2 \cdot L^2)$, coefficient $a = 1$, and the initial condition for the flow height is $H_0(x) = e^{((-(x-5)^2/100)}$, and for the discharge is $Q_0 = 0$.

Comments

The first interesting observation is that the movement speed of the height is higher in the nonlinear case. The reason behind this is that certain values such as gravity and atmospheric pressure were ignored in the linear case when β was held constant. Additionally, it seems to give a more precise description of the height H in the nonlinear example where β is not constant. The discharge Q can also be subtracted in a similar way. Figures $2.5 - 2.7$ show that even for the nonlinear scenario, the observed results seem stable.

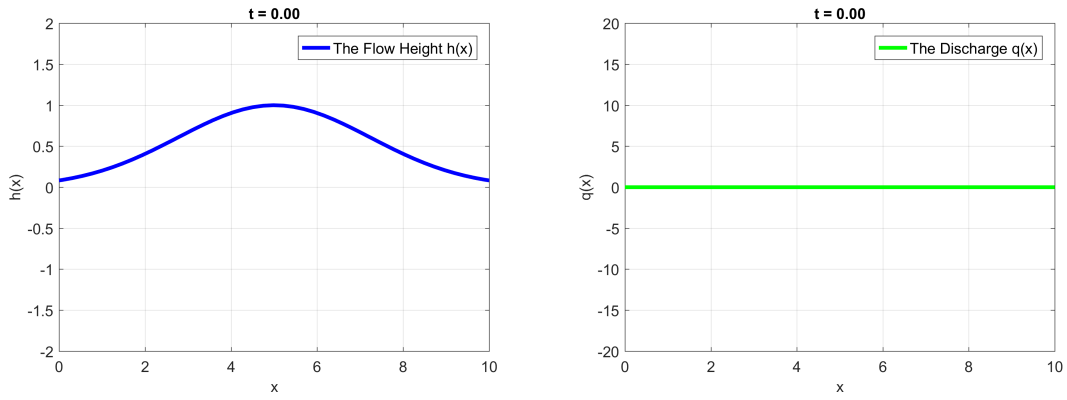

Figure 2.5: Initially the flow section for both the height H and the discharge Q.

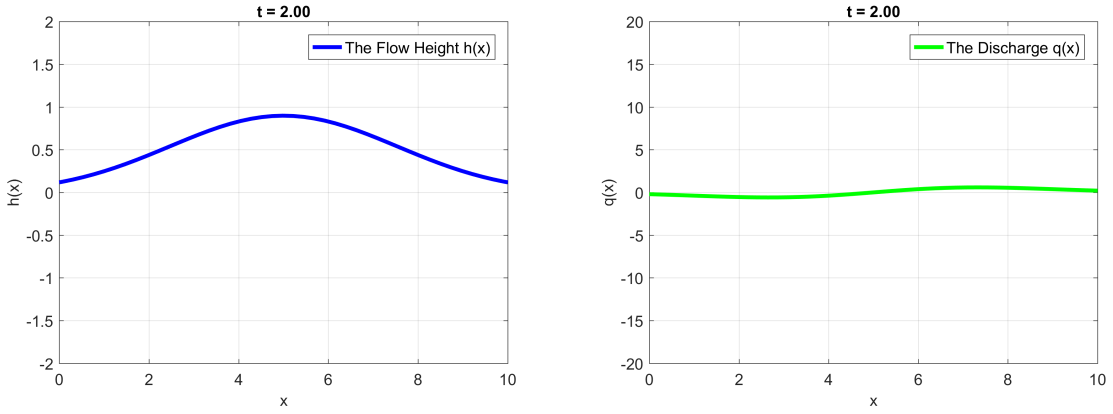

Figure 2.6: Numerical solutions of (1.1) for the height H and the discharge Q, at $t = 2$.

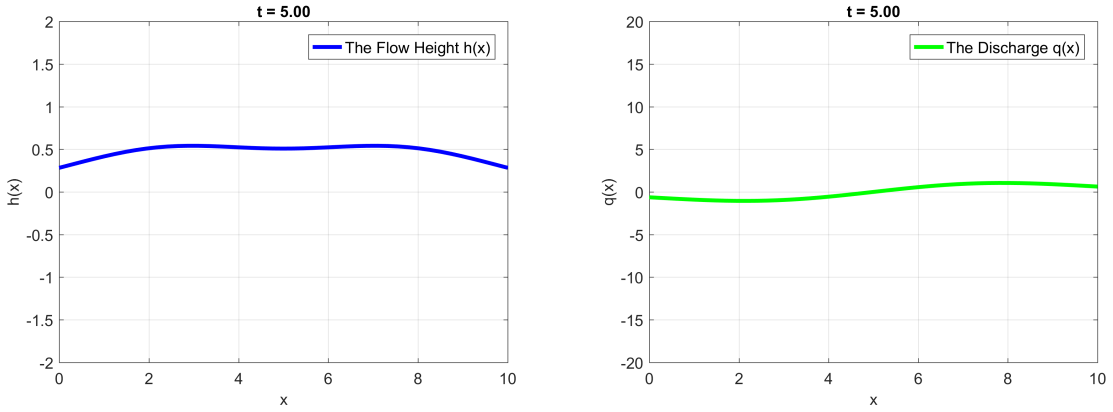

Figure 2.7: Numerical solutions of (1.1) for the height H and the discharge Q, at $t = 5$.

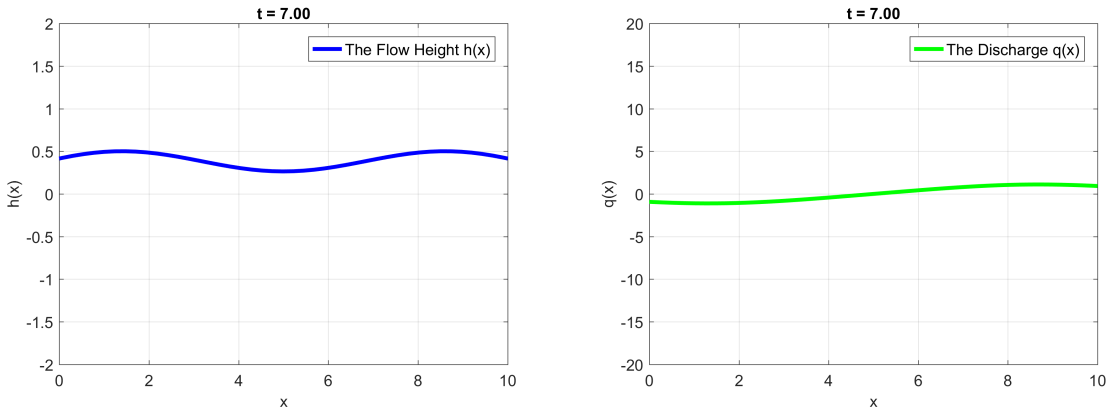

Figure 2.8: Numerical solutions of (1.1) for the height H and the discharge Q, at $t = 7$.

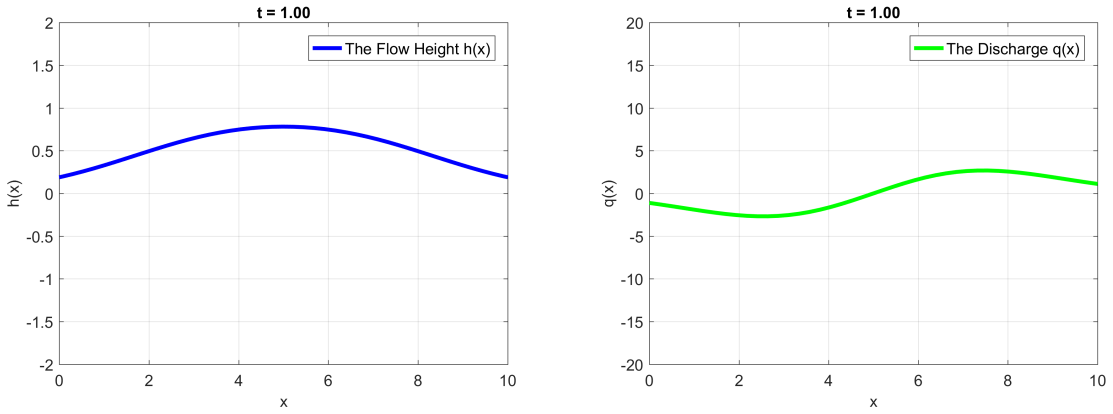

Figure 2.9: Numerical solutions of (2.2) for the height H and the discharge Q, at $t = 1$.

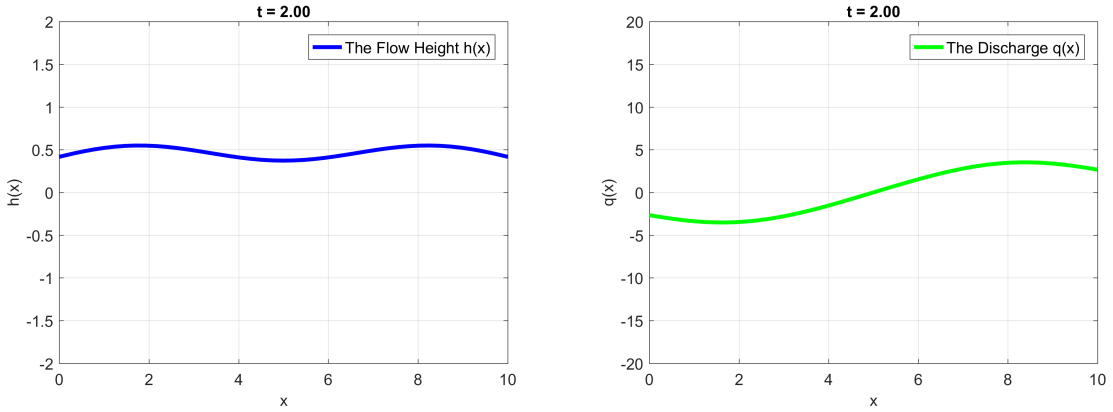

Figure 2.10: Numerical solutions of (2.2) for the height H and the discharge Q, at $t = 2$.

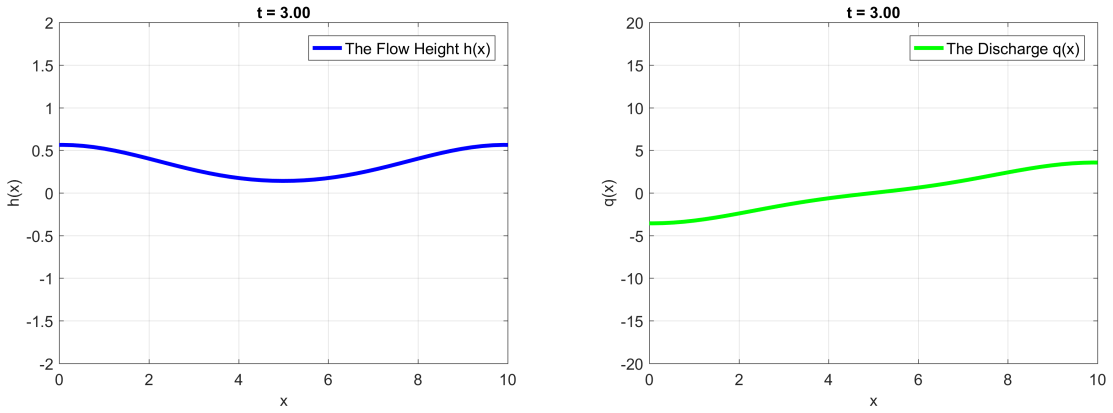

Figure 2.11: Numerical solutions of (2.2) for the height H and the discharge Q, at $t = 3$.

2.4 Conclusion

In this chapter, we were able to explore a new approach utilizing the traveling wave form to establish the well-posedness of the nonlinear SWM, employing mathematical techniques such as Schauder's fixed point theorem and the Banach contraction principle and providing an explicit solutions based on the traveling wave form. For numerical experiments, we used a forward explicit finite difference method, taking into account the stability CFL requirements (2.42) and (2.50). Resuming the numerical results for both cases instances are Figures $2.5 - 2.7$, on which the previous section provided comments. The results indicate that the model is stable in both cases.

The work of this chapter was the subject of a published paper, cited in [33].

Chapter 3

Transport of pollutant using a shallow water model

In this chapter, we focuses on studying the connection between a SWM and the T-E in order to calculate the motion of passive pollutants.
This chapter is organized in the following manner. We describe our model by adding a T-E to (2.2), then utilize the traveling wave solution to establish the well-posedness of this model. We present numerical discretizations for our model and conduct stability analysis. Numerical results and comments are provided and we finish with conclusion remark.

3.1 Proposed model

To conduct an analysis of pollutant transportation, we incorporate a third equation.

$$H\frac{\partial p}{\partial t} + Q\frac{\partial p}{\partial x} = (p_S - p)S. \tag{3.1}$$

It is a classical T-E where p is the pollution concentration, the values S and p_S are the source terms.

Let $\Omega = (0,T) \times \Gamma$, with $\Gamma = [0,L]$ such that L is positive strict, then the proposed model is one dimension presented as follows

$$\begin{cases} l\frac{\partial H}{\partial t} + \frac{\partial Q}{\partial x} = f_1, \\ \frac{\partial Q}{\partial t} - \nu\frac{\partial^2 Q}{\partial x^2} + a\frac{\partial H}{\partial x} + 2bH\frac{\partial H}{\partial x} = f_2, \\ H\frac{\partial p}{\partial t} + Q\frac{\partial p}{\partial x} = (p_S - p)S, \\ H(0,x) = H_0(x), \\ Q(0,x) = Q_0(x), \\ p(0,x) = p_0(x), \end{cases} \tag{3.2}$$

where the unknowns are the flow height H and the discharge Q. The values l and ν are the width and viscosity respectively and external forces are $f1$ and f_2.

Let $K_1, K_2 \in \mathbb{R}^*$, and we already know that H and Q should be limited, then $\forall (t,x) \in \Omega$, we get

$$\begin{aligned} \sup_{(t,x)\in\Omega} |H| \leq K_1, \\ \sup_{(t,x)\in\Omega} |Q| \leq K_2, \end{aligned} \tag{3.3}$$

Let λ be a strictly positive constant, and $\eta = x - ct$ such that $\eta \in [0,\lambda]$ and c is strictly positive constant denotes the traveling wave velocity.

we assume

$$\begin{cases} H(x,t) = \varrho(x-ct), \\ Q(x,t) = \sigma(x-ct), \\ p(x,t) = \varphi(x-ct), \end{cases} \tag{3.4}$$

Using (3.3), yields

$$\sup_{(t,x)\in\Omega} |\varrho| \leq K_1. \tag{3.5}$$

$$\sup_{(t,x)\in\Omega} |\sigma| \leq K_2. \tag{3.6}$$

By substituting (3.4) in (3.2), we get the system written as follows

$$\begin{cases} -lc\varrho'(\eta) + \sigma'(\eta) = f_1, \\ -c\sigma'(\eta) - \nu\sigma''(\eta) + (a + 2b\varrho(\eta))\varrho'(\eta) = f_2, \\ \varrho\varphi'(\eta) + \sigma\varphi'(\eta) = (p_S - \varphi(\eta))S, \\ \varrho(\eta)_{t=0} = \varrho_0, \\ \sigma(\eta)_{t=0} = \sigma_0, \\ \varphi(\eta)_{t=0} = \varphi_0. \end{cases} \tag{3.7}$$

By integrating the second equation in (3.7), we get

$$\begin{cases} \varrho'(\eta) = \dfrac{1}{lc}(\sigma'(\eta) - f_1), \\ \sigma'(\eta) = \sigma_1 + \dfrac{1}{\nu}\int_0^\eta \left(a\varrho'(\eta) + 2b\varrho(\eta)\varrho'(\eta) - c\sigma'(\eta) - f_2\right) d\eta, \quad \sigma_1 = \sigma'(0), \\ \varphi'(\eta) = S\dfrac{p_s - \varphi(\eta)}{\varrho(\eta) + \sigma(\eta)}, \\ \varrho(\eta)_{t=0} = \varrho_0 \ \ \forall x \in I, \\ \sigma(\eta)_{t=0} = \sigma_0 \ \ \forall x \in I, \\ \varphi(\eta)_{t=0} = \varphi_0 \ \ \forall x \in I. \end{cases} \tag{3.8}$$

By using fixed point theorems, we will investigate the necessary conditions for getting at least one solution, as well as its uniqueness.

3.2 Main Results

Let us present the fundamental and necessary definitions. The Banach space of continuous functions from $[0,\lambda] \longrightarrow \mathbb{R}$ with $\lambda > 0$, is denoted by $C([0,\lambda],\mathbb{R})$, with the norm

$$\|\varrho\|_\infty = \sup_{\eta\in[0,\lambda]} |\varrho|.$$

Let $u = (\varrho, \sigma, \varphi)$ be solution of

$$\begin{cases} \varrho' = \kappa_1(\eta, u(\eta)), \\ \sigma' = \kappa_2(\eta, u(\eta)), \\ \varphi' = \kappa_3(\eta, u(\eta)), \end{cases} \tag{3.9}$$

where $\kappa_{1\leq i\leq 3}(\eta, u(\eta))$ represents the right hand side of (3.8).

applying fixed-point theory , we demonstrate the existence of at least one solution of (3.8). Let $u = (\varrho, \sigma, \varphi) \in E$, such that $E = [C([0,\lambda],\mathbb{R}_+]^3$ is a Banach space equipped with the norm

$$\|u\|_E = \|\varrho\|_\infty + \|\sigma\|_\infty + \|\varphi\|_\infty,$$

and let $k = (\kappa_1, \kappa_2, \kappa_3)$ such that

$$\begin{cases} \kappa_1(\eta, u(\eta)) = \frac{1}{lc}(\sigma'(\eta) - f_1), \\ \kappa_2(\eta, u(\eta)) = \sigma_1 + \dfrac{1}{\nu}\int_0^\eta \left(a\varrho'(\eta) + 2b\varrho\varrho'(\eta) - c\sigma'(\eta) - f_2\right) d\eta, \\ \kappa_3(\eta, u(\eta)) = S\dfrac{p_s - \varphi(\eta)}{\varrho(\eta) + \sigma(\eta)}. \end{cases} \tag{3.10}$$

The function $k \in ([0,\lambda] \times E)^3$ is evidently continuous.

Applying the integral to system (3.9)'s two sides yields

$$\begin{cases} \varrho(\eta) = \varrho_0 + \int_0^\eta \kappa_1(\xi, u(\xi))d\xi, \\ \sigma(\eta) = \sigma_0 + \int_0^\eta \kappa_2(\xi, u(\xi))d\xi, \\ \varphi(\eta) = \varphi_0 + \int_0^\eta \kappa_3(\xi, u(\xi))d\xi. \end{cases} \tag{3.11}$$

By choosing $u_0 = (u_1, u_2, u_3) = (\varrho_0, \sigma_0, \varphi_0)$, we obtain

$$u(\eta) = u_0 + \int_0^\eta \kappa(\xi, u(\xi))d\xi.$$

We present the principal results written as follows:

Theorem 3.2.1 *(**Existence**) let a, b, c, K_1, K_2, L, S, ν, λ and $\mu \in \mathbb{R}_+$, with*

$$\mu = max\{\frac{1}{lc}, \frac{\lambda}{\nu}(a + 2bk_1 + c), \frac{S}{k_1 + k_2}\},$$

if

$$\mu < 1 \tag{3.12}$$

Then, there is at least one solution of (2.7) *on* $[0,\lambda]$.

Proof. Let us transform (3.8) into a fixed point problem written in the form $Fu(\eta) = u(\eta)$, with

$$Fu(\eta) = (F_1u(\eta), F_2u(\eta), F_3u(\eta)),$$

and

$$F_iu(\eta) = u_0 + \int_0^\eta \kappa_i(\xi, u(\xi))d\xi, \quad i = 1:3. \tag{3.13}$$

We prove that if $u \in E$, then $(F_i u)_{1\leq i\leq 3}$, is a continuous operator and therefore $Fu \in E$ with the norm

$$\|Fu\|_E = \sum_{i=1}^{3} \|F_i u\|_\infty.$$

Next, we prove that F satisfies the conditions of Schauder's fixed point theorem, through the following steps:

- **Step 1:** F is a nonlinear continuous operator.

  Let $(u_n)_{n\in N} = (\varrho_n, \sigma_n, \varphi)$ be three positive sequences such that $\lim\limits_{x\to+\infty} u_n = u$ in E, this implies $\lim\limits_{x\to+\infty} \varrho_n = \varrho$, $\lim\limits_{x\to+\infty} \sigma_n = \sigma$ and $\lim\limits_{x\to+\infty} \varphi_n = \varphi$ in E.
  We have already have from (2.15) and (2.16) the following inequality

$$|F_1 u_n(\eta) - F_1 u(\eta)| \leq (\frac{1}{lc})\|u_n - u\|_E.$$

$$|F_2 u_n(\eta) - F_2 u(\eta)| \leq \frac{\lambda}{\nu}(a + 2bk_1 + c)\|u_n - u\|_E.$$

  Similarly, wa have

$$\begin{array}{lll} |F_3 u_n(\eta) - F_3 u(\eta)| & = & |\int_0^\eta \kappa_3(\xi, u_n(\xi))d\xi - \int_0^\eta \kappa_3(\xi, u(\xi))d\xi|, \\ & = & |\int_0^\eta S\dfrac{p_s - \varphi_n(\eta)}{\varrho_n(\eta) + \sigma_n(\eta)} - S\dfrac{p_s - \varphi(\eta)}{\varrho(\eta) + \sigma(\eta)}d\xi, \\ \text{by using} \quad \text{(3.5) and (3.6)} & \leq & \frac{S}{K_1+K_2}\|u_n - u\|_E, \end{array}$$

  we assume that $\mu = max\{\dfrac{1}{lc}, \dfrac{\lambda}{\nu}(a + 2bK_1 + c), \dfrac{S}{K_1 + K_2}\}$, then we have

$$|F_i u_n(\eta) - F_i u(\eta)| \leq \mu\|u_n - u\|_E, \ \sigma > 0, \ i = 1:3.$$

  Since $u_n \longrightarrow u$ in E, consequently F is continuous.

- **Step 2:** $F(E_j) \subset E_j$.

Let j be a real positive number such that

$$j \geq \frac{3}{1-3\mu} u_i.$$

The subset E_j defined as follows:

$$E_j = \{u \in E : \|u\|_E \leq j\}.$$

Clearly E_j represents a closed, bounded and convex subset of E.

Let $F : E_j \to E$ be the integral operator given by (2.14), thus $F(E_j) \subset E_j$, we have

$$\begin{aligned} |F_1 u(\eta)| &\leq u_1 + \frac{1}{lc} j, \\ |F_2 u(\eta)| &\leq u_2 + \frac{1}{\nu}(\frac{\lambda}{\nu_S}(a + 2bK_1 + c)j, \\ |F_3 u(\eta)| &\leq u_3 + \frac{}{K_1 + K_2} j. \end{aligned} \tag{3.14}$$

Thus, in each case, we get

$$\begin{aligned} |F_i u(\eta)| &\leq u_i + \mu j, \\ &\leq \frac{1-3\mu}{3} j + \mu j, \\ &\leq \frac{1}{3} j, \quad i = 1:3, \end{aligned} \tag{3.15}$$

or $(\|F_i u\|_\infty)_{1 \leq i \leq 3} \leq \frac{j}{3}$, then

$$\|Fu\|_E = \sum_{i=1}^{3} \|F_i u\|_\infty \leq j.$$

Consequently $F(E_j) \subset E_j$.

- **Step 3:** $F(E_j)$ is relatively compact. Let $\eta_1, \eta_2 \in [0, \lambda], \eta_1 < \eta_2$ and $u \in E_j$, we obtain

from (2.20) and (2.21) that

$$|F_1u(\eta_1) - F_1u(\eta_2)| \leq 0. \tag{3.16}$$

$$|F_2u(\eta_1) - F_2u(\eta_2)| \leq 0. \tag{3.17}$$

Similarly, we can find that

$$|F_3u(\eta_1) - F_3u(\eta_2)| \leq 0. \tag{3.18}$$

Then from (3.16), (3.17) and (3.18) we obtain

$$|F_iu(\eta_1) - F_iu(\eta_2)| \leq 0, \quad i = 1:3. \tag{3.19}$$

Based on steps 1–3 and the Ascoli-Arzela theorem, we may certainly state the continuity and compactness of $F : E_j \to E_j$. This indicates that F satisfies Schauder's fixed point theorem [25]. Thus, F has a fixed-point solution of (3.8) on $[0, \lambda]$.In Theorem 3.2.1, we established that (3.8) has at least one possible solution. If Theorem 3.2.1 holds for all $(x, t) \in \Omega$, then there is at least one solution of (3.2) under the traveling wave form (3.4).

Theorem 3.2.2 *(**Uniqueness**) let a, b, c, K_1, k_2, L, S, ν, λ and $\mu \in \mathbb{R}_+$,with*

$$\mu = max\{\frac{1}{lc}, \frac{\lambda}{\nu}(a + 2bK_1 + c), \frac{S}{K_1 + K_2}\},$$

if

$$\mu < 1, \tag{3.20}$$

then, (3.8) *admits a unique solution on* $[0, \lambda]$.

Proof. In Theorem 3.2.1., We have already transformed (3.8) into a fixed point problem. Let $u, v \in E$ satisfy (3.8). This implies that:

$$\begin{aligned} |F_1u(\eta) - F_1v(\eta)| &\leq \frac{1}{lc}\|u - v\|_E, \\ |F_2u(\eta) - F_2v(\eta)| &\leq \frac{\lambda}{\nu}(a + 2bK_1 + c)\|u - v\|_E, \\ |F_3u(\eta) - F_3v(\eta)| &\leq \frac{S}{K_1 + k_2}\|u - v\|_E, \end{aligned} \tag{3.21}$$

we assume that $\mu = max\{\frac{1}{lc}, \frac{\lambda}{\nu}(a + 2bK_1 + c), \frac{S}{K_1 + K_2}\}$, then we have

$$\|F_iu - F_iv\|_\infty \leq \mu\|u - v\|_E.$$

Similarly, we can find that:

$$\|Fu - Fv\|_E \leq \mu\|u - v\|_E. \tag{3.22}$$

Based on Theorem 3.2.1., and inequality (3.22), it can be established that F is indeed a contraction. Deriving from Banach's contraction principle (refer to [25]), it is apparent that F possesses a fixed point which is the unique solution for (3.8) within the interval $[0, \lambda]$. According Theorem 3.2.2., there is a unique solution of (3.2) if (3.20) holds.

3.2.1 Explicit Solution

We already obtained the solution for the first two equation of , and by substitute (2.34) and (2.35) in the third equation of (3.8), we obtain

$$\varphi'(\eta) = \frac{-\varphi(\eta)}{\frac{\alpha - \kappa\beta e^{(\alpha-\beta)\eta}}{1 - \kappa\beta e^{(\alpha-\beta)\eta}} + \frac{\alpha - \kappa\beta e^{(\alpha-\beta)\eta}}{lc(1 - \kappa\beta e^{(\alpha-\beta)\eta})}}, \tag{3.23}$$

this implies

$$\varphi'(\eta) = \frac{-\varphi(\eta)}{(1+\frac{1}{lc})\frac{\alpha-\kappa\beta e^{(\alpha-\beta)\eta}}{1-\kappa\beta e^{(\alpha-\beta)\eta}}}. \tag{3.24}$$

To solve (3.24), we start by simplifying the equation. First, define the constant $k = 1 + \frac{1}{lc}$, this implies

$$\frac{d\varphi(\eta)}{\varphi(\eta)} = -\frac{1}{k}.\frac{1-\kappa\beta e^{(\alpha-\beta)\eta}}{\alpha-\kappa\beta e^{(\alpha-\beta)\eta}}. \tag{3.25}$$

Integrate both sides

$$ln|\varphi(\eta)| = -\frac{1}{k}\int \frac{1-\kappa\beta e^{(\alpha-\beta)\eta}}{\alpha-\kappa\beta e^{(\alpha-\beta)\eta}} d\eta. \tag{3.26}$$

This implies that the explicit solution of the third equation of (3.8) written as follows

$$\varphi(\eta) = C_2|\alpha-\kappa\beta e^{(\alpha-\beta)\eta}|^{-\frac{1}{\kappa\alpha}}, \tag{3.27}$$

where C_2 is a positive constant.

From (3.27) we can find that

$$p(x,t) = C_2|\alpha-\kappa\beta e^{(\alpha-\beta)(x-ct)}|^{-\frac{1}{\kappa\alpha}}, \tag{3.28}$$

Figures $3.1 - 3.4$ show the variations of an explicit solutions for the height H, discharge Q and pollution p, presented as follows:

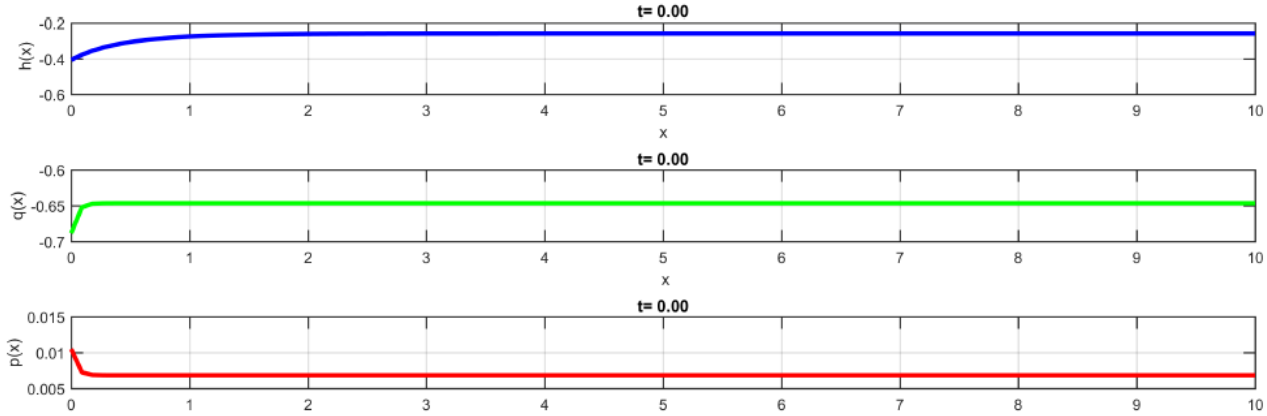

Figure 3.1: Initial solutions for the height H and the discharge Q.

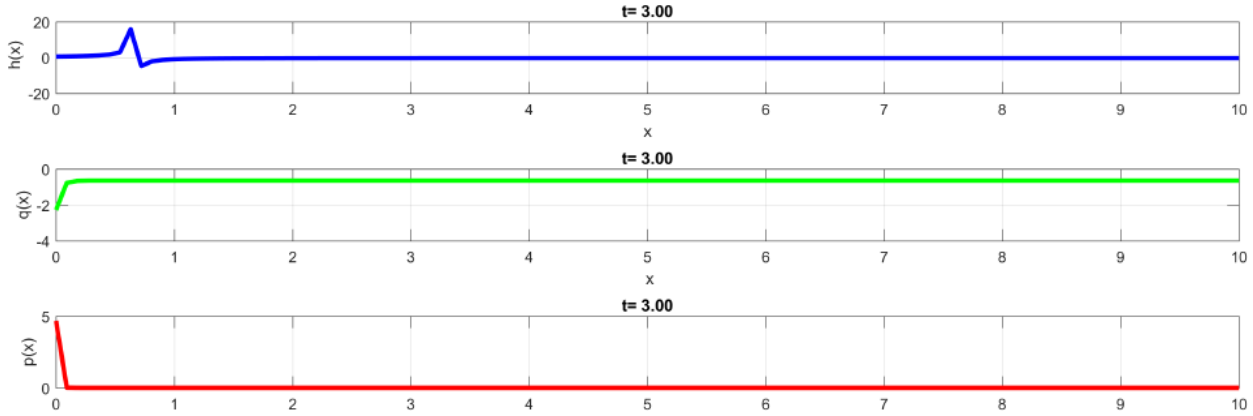

Figure 3.2: Solutions of (3.2) for the height H, the discharge Q and pollution concentration, at $t = 3$.

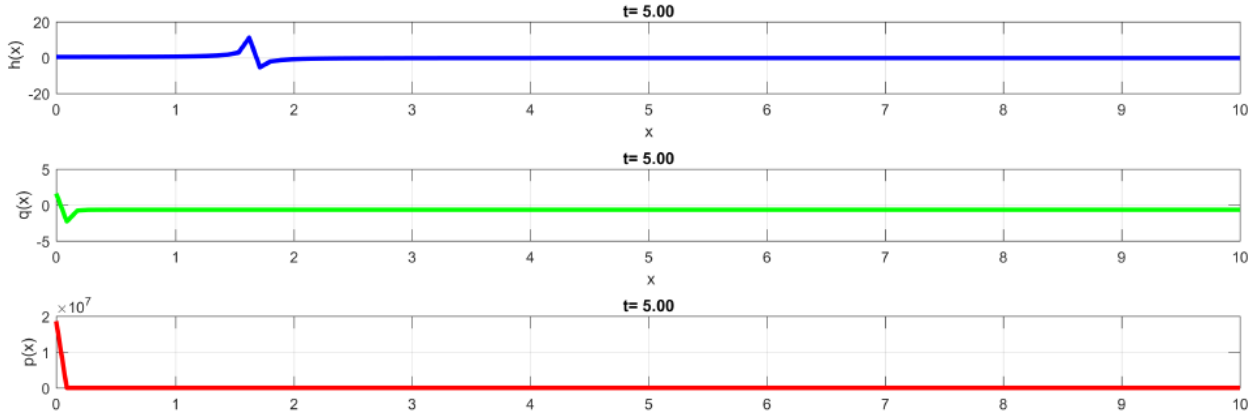

Figure 3.3: Solutions of (3.2) for the height H, the discharge Q and pollution concentration, at $t = 5$.

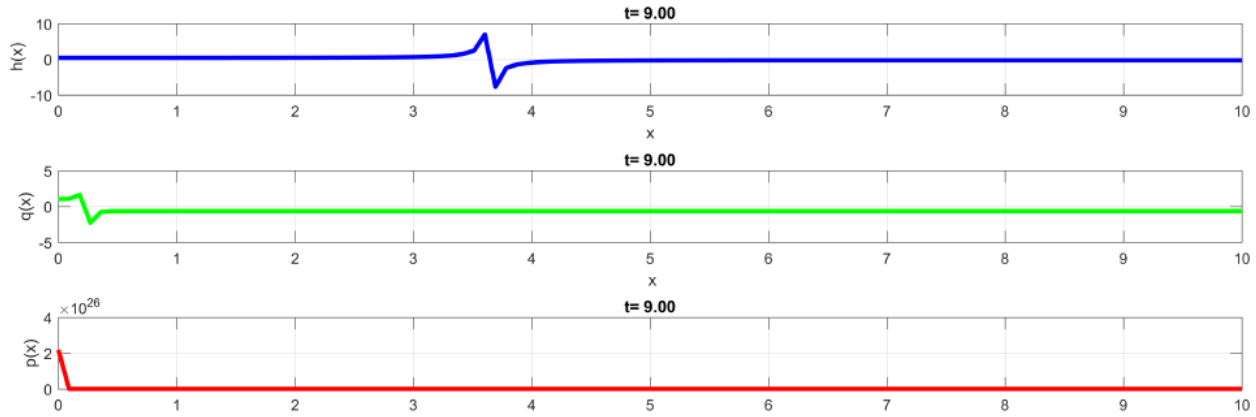

Figure 3.4: Solutions of (3.2) for the height H, the discharge Q and pollution concentration, at $t = 9$.

Comment

The parameters of (2.34), (2.35) and (3.28) are chosen adaptively and presented as follows: the traveling wave velocity $c = 12$, the width $l = 5$, the values $C_0 = 1/8$,$C_1 = 1$ and $C_2 = 1$. The obtained results from these solutions are resumed in Figures $3.1 - 3.4$ which demonstrate the variations of the flow height H, discharge Q, and pollution p. We observe a decreasing solution behavior for each of these quantities. the variation of the flow height H with respect to x at $t = 1, 3, 5$ and 9 decreases smoothly as x increases, indicating a stable wave propagation. The discharge Q exhibits a similar decreasing trend as the flow height H. This consistency suggests that the flow characteristics are maintained uniformly over the spatial domain, contributing to the overall stability of the ow wave.

The pollution p also shows a decreasing behavior with x. The exponential decay implies that the pollution levels reduce signicantly as the wave travels.

3.3 Numerical Approximation

In this part, we discretize (3.2) with $f = 0$ and establish a stability condition for the proposed numerical method.

3.3.1 Finite difference approximation

We use an explicit finite difference approach to discretize (3.2). The temporal and spatial derivatives expressed in (2.36) and (2.37). The first two equations of (3.2) discretized in (2.40) and (2.41). Then, we obtain $H_i^{n+1}$and Q_i^{n+1} p_i^{n+1}:

$$H_i^{n+1} = H_i^n - \frac{\Delta t}{l}\left(\frac{Q_{i+1}^n - Q_{i-1}^n}{2\Delta x}\right). \tag{3.29}$$

$$\begin{aligned} Q_i^{n+1} &= Q_i^n - \Delta t\left(-\nu\left(\frac{Q_{i+1}^n - 2Q_i^n + Q_{i-1}^n}{(\Delta x)^2}\right) - a\left(\frac{H_{i+1}^n - H_{i-1}^n}{2\Delta x}\right)\right) \\ &- \Delta t b H_i^n\left(\frac{H_{i+1}^n - H_{i-1}^n}{2\Delta x}\right). \end{aligned} \tag{3.30}$$

$$p_i^{n+1} = p_i^n - \frac{\Delta t}{h_i^n}\left(q_i^n\frac{p_{i+1}^n - p_{i-1}^n}{2\Delta x} - (p_s - p_i^n)S\right). \tag{3.31}$$

3.3.2 Stability analysis

We establish a result concerning the numerical stability of (3.29)-(3.31) and present its numerical implementation.

We already proved the stability for (3.29) and (3.30) in 2.3.1. and 2.3.2.

Proposition 3.3.1 *Numerical scheme* (3.31) *is stable under the following conditions:*

$$\Delta t \leq \frac{(1+S)H_m\Delta x}{Q_m}, \tag{3.32}$$

with $H_m = max(h_j^n)$ *and* $Q_m = max(q_j^n)$.

Proof. Similarly, using the same procedure as in Proposition 2.3.1, and we can find that:

$$\Delta t \leq \frac{(1+S)H_m \Delta x}{Q}.$$

3.3.3 Numerical results and comments

We apply the following algorithm to solve (3.29)-(3.31) numerically:

Algorithm 3.3.2

- *Step 1 (Initialization): input the gravity g, length L and width l, viscosity ν, coefficients a and b, space step Δx, time step Δt, final time T and the starting solution for the height H_0, discharge Q_0 and pollution p_0.*
- *Step 2: solve* (3.29) *for the flow height H.*
- *Step 3: solve* (3.30) *for the flow discharge Q.*
- *Step 4: solve* (3.31) *for the pollution p.*
- *Repeat steps 2-4 until T is reached.*

The results obtained for solving (3.2) are summarized in Figures 3.1 and 3.2, illustrating the changes in height H, discharge Q and the propagation of pollution p at different times t. The discretization parameters have been set as follows: $\Delta x = 0.3$, Δt has been chosen in accordance with the stability CFL conditions. The dimensions are: length $L = 1$, width $l = 5$, source term $S = 0.1$, value of the pollutant concentration $p_S = 10$, viscosity $\nu = 5 * 10^{-3}$, the coefficients are calculated as $b = l^2 \cdot g \cdot T^2/(2 \cdot L^2)$ and $a = 1$.
The initial condition are expressed as:

$$H_0(x) = e^{((-(x-5)^2/100)}, \tag{3.33}$$

$$Q_0 = 0, \tag{3.34}$$

$$p_0 = 1. \tag{3.35}$$

Figures 3.5 – 3.6 show the numerical solutions of (3.2) for the flow height H, discharge Q and pollution p, presented as follows:

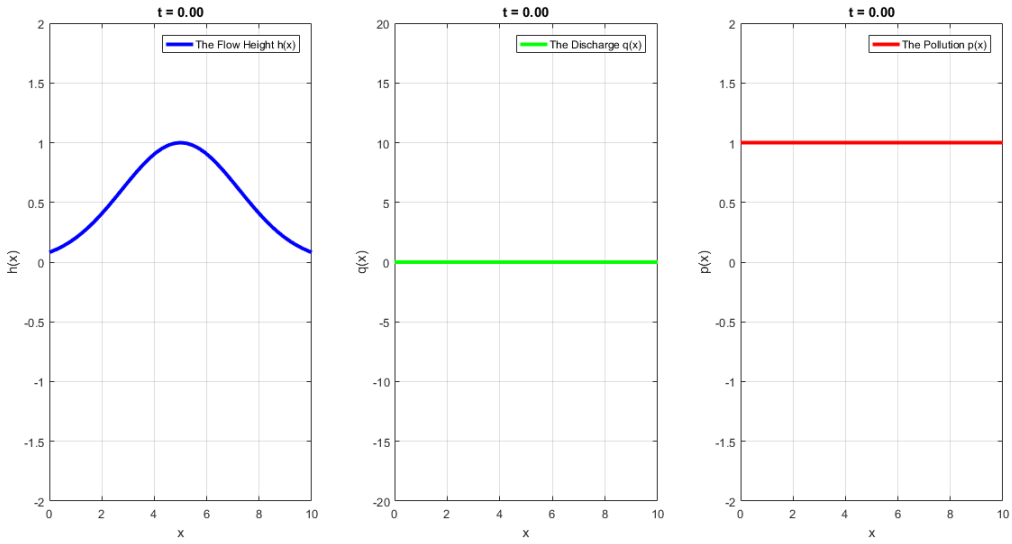

Figure 3.5: Initially the flow section for the height h, the discharge q and the pollution p.

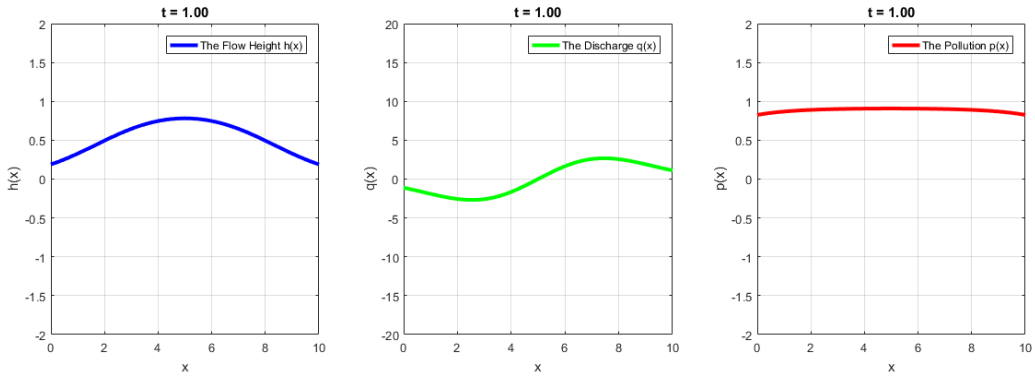

Figure 3.6: Numerical solutions of (3.2) for the height h, the discharge q and the pollution p, at time $t = 1$.

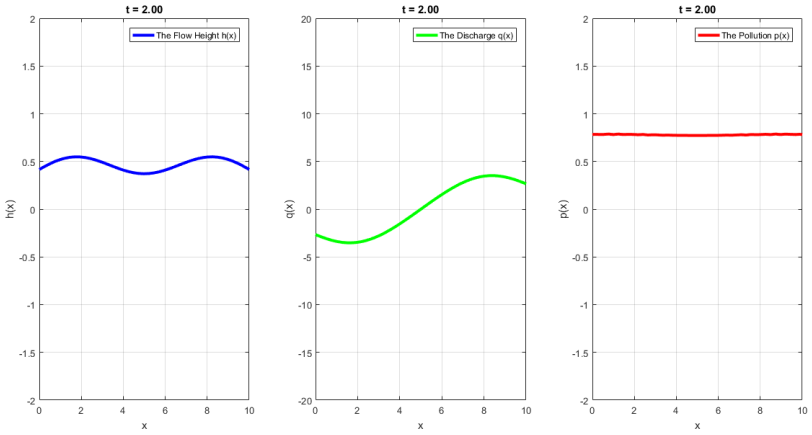

Figure 3.7: Numerical solutions of (3.2) for the height h, the discharge q and the pollution p, at time $t = 2$.

Comments

The numerical results show the motion variations in the height H, discharge Q and the propagation of pollution p over time t, we observe decreasing solutions behavior for each one at different times t. This illustrates to us how waves propagate with a decrease in height over time t. The results obtained demonstrate stability, as depicted in Figures $3.5 - 3.7$.

3.4 Conclusion

In this chapter, we studied the coupled nonlinear SWM with T-E to conduct an analysis of pollution propagation. We successfully established the well-posedness of the model, employing fundamental mathematical tools such as Schauder's fixed point theorem and the Banach contraction principle, providing an explicit solutions and the results are summarized in Figures $3.1 - 3.4$. For numerical experiments, we utilized a forward explicit finite difference method while adhering to stability conditions. Based on the results, which are summarized in figures $3.5 - 3.7$, we can infer that the model maintains stability. The work of this chapter was the subject of a submitted paper.

Chapter 4

Transport of pollutant using a regularisation of the Saint-Venant system

In this chapter, we examine a model that regularizes the SV-S coupled with a T-E to describe the pollution probagation. Firt, we define our model then present theoretical results on its well-posedness utilizing a kinetic approach. Subsequently, we explore the discretizations of the proposed model using a stable finite difference scheme in both temporal and spatial domains, then present numerical results and comments, we finish with concluding remark.

4.1 Model description

Let $\Omega = (0,T) \times I$ be a domain, such that I is a closed bounded domain in $\mathbb{R}^2$ and $T > 0$. We consider the following model

$$\begin{cases} \dfrac{\partial h}{\partial t} + div(hU) = S, \\ \dfrac{\partial hU}{\partial t} + div(hU \otimes U) + \nabla(\dfrac{g}{2}h^2) + \nabla(\epsilon R h^2) + gh\nabla Z = 0, \\ \dfrac{\partial hc}{\partial t} + div(hUc) = c_S S, \\ h(0,x,y) = h_0(x,y), \\ U(0,x,y) = U_0(x,y), \\ c(0,x,y) = c_0(x,y), \end{cases} \tag{4.1}$$

where $R = (R_1, R_2)$, such that

$$\begin{pmatrix} R_1 \\ R_2 \end{pmatrix} = \begin{pmatrix} h((\frac{\partial u}{\partial x})^2 - \frac{\partial u_t}{\partial x} - u\frac{\partial^2 u}{\partial x^2}) - g(h\frac{\partial^2 h}{\partial x^2} + \frac{1}{2}(\frac{\partial h}{\partial x})^2) \\ h((\frac{\partial v}{\partial y})^2 - \frac{\partial v_t}{\partial y} - v\frac{\partial^2 v}{\partial y^2}) - g(h\frac{\partial^2 h}{\partial y^2} + \frac{1}{2}(\frac{\partial h}{\partial y})^2) \end{pmatrix}, \tag{4.2}$$

The unknowns are the flow height $h(t,x,y) > 0$, the velocity $U = (u,v) \in \mathbb{R}^2$ for both directions (x,y), the pollutant concentration $c(t,x,y)$. The gravity is g, the given source term are S and c_S, the function $Z(x,y)$ representing the bottom topography and ϵ is a regularized parameter with $(0 < \epsilon < 1)$.

The first two equations of (4.1) represent a regularized version of the SV-S while the third one is the classical T-E.

We can write this system in the conservative and compact form

$$\frac{\partial \varphi}{\partial t} + divF(\varphi) = B(\varphi), \tag{4.3}$$

with $\varphi = \begin{pmatrix} h \\ q \\ e \end{pmatrix}$, $F(\varphi) = \begin{pmatrix} q \\ \frac{q\otimes q}{h} + \frac{gh^2}{2} Id + \epsilon R h^2 \\ \frac{qe}{h} \end{pmatrix}$, $B(\varphi) = \begin{pmatrix} S \\ -gh\nabla Z \\ c_S S \end{pmatrix}$,
such that the discharge is $q = hU$ and the quantity of pollutant is denoted by $e = hc$.

4.1.1 Main Results

Here, we present a dynamic approach to (4.1) in homogeneous case, i.e $S = 0$.

Let $\chi(w)$ be an even and compactly supported probability defined on R^2 satisfying

$$\int_{R^2} \begin{pmatrix} 1 \\ w_i w_j \end{pmatrix} \chi(w) dw = \begin{pmatrix} 1 \\ \delta_{ij} \end{pmatrix}, \tag{4.4}$$

In addition we assume that $\chi(w)$ is compactly supported, i.e.

$$\exists w_M \in R, such \ \ that \quad \chi(w) = 0 \quad for \quad |w| \geq w_M.$$

We introduce two microscopic densities of particles $M(t, x, \xi)$ and $N(t, x, \xi)$ defined by a Gibbs equilibrium

$$M(t, x, y, \xi) = \frac{h(t, x, y)}{c(t, x, y)} \chi\left(\frac{\xi - U(x, y)}{c(t, x, y)}\right),$$

$$N(t, x, y, \xi) = \frac{e(t, x, y)}{c(t, x, y)} \chi\left(\frac{\xi - U(x, y)}{c(t, x, y)}\right),$$

$$c(t, x, y)^2 = h(t, x, y)\left(\frac{g}{2} Id + \epsilon R(t, x, y)\right).$$

We denote by

$$G(t, x, y, \xi) = \begin{pmatrix} M(t, x, y, \xi) \\ N(t, x, y, \xi) \end{pmatrix}.$$

Theorem 4.1.1 *The functions* (h, q, e) *are weak solution of* (4.3) *if and only if* $G(t, x, y, \xi)$ *is solution of the kinetic equation*

$$\frac{\partial G}{\partial t} + \xi \cdot \nabla G - g \nabla Z \nabla_\xi G = Q(t, x, y, \xi), \tag{4.5}$$

where, $Q(t, x, y, \xi) = \begin{pmatrix} Q_1(t, x, y, \xi) \\ Q_2(t, x, y, \xi) \end{pmatrix}$, *is a collision term satisfying*

$$\int_{R^2} \begin{pmatrix} 1 \\ \xi \end{pmatrix} Q_1 d\xi = 0, \quad \int_{R^2} Q_2 d\xi = 0. \tag{4.6}$$

Proof. System (4.3) are equivalent to (4.1) once integrated in ξ against $K(\xi)$ such that

$$K(\xi) = \begin{pmatrix} 1 & 0 \\ \xi & 0 \\ 0 & 1 \end{pmatrix}. \tag{4.7}$$

If we multiply (4.7) by (4.5) we obtain the following system

$$\begin{cases} \frac{\partial M}{\partial t} + \xi \cdot \nabla M - g \nabla z \nabla_\xi M = Q_1(t, x, y, \xi), \\ \xi \frac{\partial M}{\partial t} + \xi \otimes \xi \nabla M + \xi \nabla z \nabla_\xi M = \xi Q_1(t, x, y, \xi), \\ \frac{\partial N}{\partial t} + \xi \cdot \nabla N - g \nabla z \nabla_\xi N = Q_2(t, x, y, \xi), \end{cases} \tag{4.8}$$

By integrating (4.8) in ξ and we use the properties of χ in (4.4) we deduce:

$$\begin{pmatrix} h \\ q \\ \frac{q\otimes q}{h} + h^2\left(\frac{g}{2}Id + \epsilon R\right) \end{pmatrix} = \int_{R^2} \begin{pmatrix} 1 \\ \xi \\ \xi \otimes \xi \end{pmatrix} M(\xi) d\xi$$

$$\begin{pmatrix} e \\ \frac{qe}{h} \end{pmatrix} = \int_{R^2} \begin{pmatrix} 1 \\ \xi \end{pmatrix} N(\xi) d\xi$$

$$\begin{pmatrix} 0 \\ h \\ 0 \end{pmatrix} = -\int_{R^2} K(\xi) \nabla_\xi G(\xi) d\xi.$$

We can refer to to [42] for more understanding and details of the hydrodynamic element of the kinetic interpretation, and [5] for the handling of the source term at this microscopic level.

4.2 Numerical Approximation

In this part, we discretize (4.1) with $S = 0$ and establish a stability condition for the proposed numerical method.

4.2.1 Finite difference approximation

We use an explicit finite difference approach to discretize (4.1). The temporal and spatial derivatives are defined as follows:

$$\frac{\partial u}{\partial t} = \frac{u_{i,j}^{n+1} - u_{i,j}^{n}}{\Delta t}, \quad \frac{\partial u}{\partial x} = \frac{u_{i+1,j}^{n} - u_{i-1,j}^{n}}{2\Delta x}, \quad \frac{\partial u}{\partial y} = \frac{u_{i,j+1}^{n} - u_{i,j-1}^{n}}{2\Delta y}. \tag{4.9}$$

Thus, we get

$$\begin{cases} \frac{h_{i,j}^{n+1}-h_{i,j}^{n}}{\Delta t} &= S - u_{i,j}^{n}\frac{h_{i+1,j}^{n}-h_{i-1,j}^{n}}{2\Delta x} - h_{i,j}^{n}\frac{u_{i+1,j}^{n}-u_{i-1,j}^{n}}{2\Delta x} - v_{i,j}^{n}\frac{h_{i,j+1}^{n}-h_{i,j-1}^{n}}{2\Delta y} \\ &- h_{i,j}^{n}\frac{v_{i,j+1}^{n}-v_{i,j-1}^{n}}{2\Delta y}, \end{cases} \tag{4.10}$$

$$\begin{cases} h_{i,j}^{n}\frac{u_{i,j}^{n+1}-u_{i,j}^{n}}{\Delta t} = -u_{i,j}^{n}\frac{h_{i,j}^{n+1}-h_{i,j}^{n}}{\Delta t} - (u_{i,j}^{n})^{2}\frac{h_{i+1,j}^{n}-h_{i-1,j}^{n}}{2\Delta x} - u_{i,j}^{n}h_{i,j}^{n}\frac{u_{i+1,j}^{n}-u_{i-1,j}^{n}}{\Delta x} \\ -gh_{i,j}^{n}\frac{h_{i+1,j}^{n}-h_{i-1,j}^{n}}{2\Delta x} - \epsilon h_{i,j}^{n}R_{i,j}^{n}\frac{h_{i+1,j}^{n}-h_{i-1,j}^{n}}{\Delta x} - \epsilon(h_{i,j}^{n})^{2}\frac{(R_1)_{i+1,j}^{n}-(R_1)_{i-1,j}^{n}}{2\Delta x} \\ -h_{i,j}^{n}u_{i,j}^{n}\frac{v_{i,j+1}^{n}-v_{i,j-1}^{n}}{2\Delta y} - h_{i,j}^{n}v_{i,j}^{n}\frac{u_{i,j+1}^{n}-u_{i,j-1}^{n}}{2\Delta y} - v_{i,j}^{n}u_{i,j}^{n}\frac{h_{i,j+2}^{n}-h_{i,j-1}^{n}}{2\Delta y} \\ -gh_{i,j}^{n}\dfrac{\partial Z}{\partial x}, \end{cases} \tag{4.11}$$

where

$$\begin{aligned} R_1(i,j) &= h_{i,j}^{n}\left(\frac{u_{i+1,j}^{n}-u_{i-1,j}^{n}}{2\Delta x}\right)^{2} - h_{i,j}^{n}u_{i,j}^{n}\frac{u_{i+1,j}^{n}-2u_{i,j}^{n}+u_{i-1,j}^{n}}{\Delta x^{2}} \\ &- h_{i,j}^{n}\frac{u_{i+1,j}^{n+1}-u_{i-1,j}^{n+1}-u_{i+1,j}^{n}+u_{i-1,j}^{n}}{2\Delta x\Delta t} - \frac{g}{2}\left(\frac{h_{i+1,j}^{n}-h_{i-1,j}^{n}}{2\Delta x}\right)^{2} \\ &- gh_{i,j}^{n}\frac{h_{i+1,j}^{n}-2h_{i,j}^{n}+h_{i-1,j}^{n}}{\Delta x^{2}}, \end{aligned} \tag{4.12}$$

$$\begin{cases} h_{i,j}^{n}\frac{v_{i,j}^{n+1}-v_{i,j}^{n}}{\Delta t} = -v_{i,j}^{n}\frac{h_{i,j}^{n+1}-h_{i,j}^{n}}{\Delta t} - (v_{i,j}^{n})^{2}\frac{h_{i,j+1}^{n}-h_{i,j-1}^{n}}{2\Delta y} - v_{i,j}^{n}h_{i,j}^{n}\frac{v_{i,j+1}^{n}-u_{i,j-1}^{n}}{\Delta y} \\ -gh_{i,j}^{n}\frac{h_{i,j+1}^{n}-h_{i,j-1}^{n}}{2\Delta y} - \epsilon h_{i,j}^{n}R_{i,j}^{n}\frac{h_{i,j+1}^{n}-h_{i,j-1}^{n}}{\Delta y} - \epsilon(h_{i,j}^{n})^{2}\frac{(R_2)_{i,j+1}^{n}-(R_2)_{i,j-1}^{n}}{2\Delta y} \\ -h_{i,j}^{n}u_{i,j}^{n}\frac{v_{i+1,j}^{n}-v_{i-1,j}^{n}}{2\Delta x} - h_{i,j}^{n}v_{i,j}^{n}\frac{u_{i+1,j}^{n}-u_{i-1,j}^{n}}{2\Delta x} - v_{i,j}^{n}u_{i,j}^{n}\frac{h_{i+1,j}^{n}-h_{i-1,j}^{n}}{2\Delta x} \\ -gh_{i,j}^{n}\dfrac{\partial Z}{\partial y}, \end{cases} \tag{4.13}$$

where

$$\begin{aligned} R_2(i,j) &= h_{i,j}^{n}\left(\frac{v_{i,j+1}^{n}-v_{i,j-1}^{n}}{2\Delta y}\right)^{2} - h_{i,j}^{n}v_{i,j}^{n}\left(\frac{v_{i,j+1}^{n}-2v_{i,j}^{n}+v_{i,j-1}^{n}}{\Delta y^{2}}\right) \\ &- h_{i,j}^{n}\frac{v_{i,j+1}^{n+1}-v_{i,j-1}^{n+1}-v_{i,j+1}^{n}+v_{i,j-1}^{n}}{2\Delta y\Delta t} - \frac{g}{2}\left(\frac{h_{i,j+1}^{n}-h_{i,j-1}^{n}}{2\Delta y}\right)^{2} \\ &+ gh_{i,j}^{n}\frac{h_{i,j+1}^{n}-2h_{i,j}^{n}+h_{i,j-1}^{n}}{\Delta y^{2}}, \end{aligned} \tag{4.14}$$

$$\left\{\begin{array}{l} h_{i,j}^n \frac{c_{i,j}^{n+1}-c_{i,j}^n}{\Delta t} = c_S S - c_{i,j}^n \frac{h_{i,j}^{n+1}-h_{i,j}^n}{\Delta t} - h_{i,j}^n u_{i,j}^n \frac{c_{i+1,j}^n - C_{i-1,j}^n}{2\Delta x} \\ -h_{i,j}^n c_{i,j}^n \frac{u_{i+1,j}^n - u_{i-1,j}^n}{2\Delta x} - c_{i,j}^n u_{i,j}^n \frac{h_{i+1,j}^n - h_{i-1,j}^n}{2\Delta x} - h_{i,j}^n v_{i,j}^n \frac{c_{i,j+1}^n - c_{i,j-1}^n}{2\Delta y} \\ -h_{i,j}^n c_{i,j}^n \frac{v_{i,j+1}^n - v_{i,j-1}^n}{2\Delta y} - c_{i,j}^n v_{i,j}^n \frac{h_{i,j+1}^n - h_{i,j-1}^n}{2\Delta y}, \end{array}\right. \tag{4.15}$$

then, we obtain $h_{i,j}^{n+1}$, $u_{i,j}^{n+1}$ $v_{i,j}^{n+1}$ and $c_{i,j}^{n+1}$:

$$\begin{array}{rcl} h_{i,j}^{n+1} & = & h_{i,j}^n - \Delta t \left(u_{i,j}^n \frac{h_{i+1,j}^n - h_{i-1,j}^n}{2\Delta x} + h_{i,j}^n \frac{u_{i+1,j}^n - u_{i-1,j}^n}{2\Delta x} \right) \\ & - & \Delta t \left(h_{i,j}^n \frac{v_{i,j+1}^n - v_{i,j-1}^n}{2\Delta y} + v_{i,j}^n \frac{h_{i,j+1}^n - h_{i,j-1}^n}{2\Delta y} - S \right), \end{array} \tag{4.16}$$

$$\begin{array}{l} u_{i,j}^{n+1} = u_{i,j}^n - \frac{\Delta t}{h_{i,j}^n} \left(u_{i,j}^n \frac{h_{i,j}^{n+1} - h_{i,j}^n}{\Delta t} + (u_{i,j}^n)^2 \frac{h_{i+1,j}^n - h_{i-1,j}^n}{2\Delta x} \right) \\ -\frac{\Delta t}{h_{i,j}^n} \left(u_{i,j}^n h_{i,j}^n \frac{u_{i+1,j}^n - u_{i-1,j}^n}{\Delta x} g h_{i,j}^n \frac{h_{i+1,j}^n - h_{i-1,j}^n}{2\Delta x} + \epsilon h_{i,j}^n R_{i,j}^n \frac{h_{i+1,j}^n - h_{i-1,j}^n}{\Delta x} \right) \\ -\frac{\Delta t}{h_{i,j}^n} \left(\epsilon (h_{i,j}^n)^2 \frac{(R_1)_{i+1,j}^n - (R_1)_{i-1,j}^n}{2\Delta x} + h_{i,j}^n u_{i,j}^n \frac{v_{i,j+1}^n - v_{i,j-1}^n}{2\Delta y} \right) \\ -\frac{\Delta t}{h_{i,j}^n} \left(h_{i,j}^n v_{i,j}^n \frac{u_{i,j+1}^n - u_{i,j-1}^n}{2\Delta y} + v_{i,j}^n u_{i,j}^n \frac{h_{i,j+1}^n - h_{i,j-1}^n}{2\Delta y} + g h_{i,j}^n \frac{\partial Z}{\partial x} \right), \end{array} \tag{4.17}$$

$$\begin{array}{l} v_{i,j}^{n+1} = v_{i,j}^n - \frac{\Delta t}{h_{i,j}^n} \left(v_{i,j}^n \frac{h_{i,j}^{n+1} - h_{i,j}^n}{\Delta t} + (v_{i,j}^n)^2 \frac{h_{i,j+1}^n - h_{i,j-1}^n}{2\Delta y} \right) \\ -\frac{\Delta t}{h_{i,j}^n} \left(v_{i,j}^n h_{i,j}^n \frac{v_{i,j+1}^n - u_{i,j-1}^n}{\Delta y} + g h_{i,j}^n \frac{h_{i,j+1}^n - h_{i,j-1}^n}{2\Delta y} + \epsilon h_{i,j}^n R_{i,j}^n \frac{h_{i,j+1}^n - h_{i,j-1}^n}{\Delta y} \right) \\ -\frac{\Delta t}{h_{i,j}^n} \left(\epsilon (h_{i,j}^n)^2 \frac{(R_2)_{i,j+1}^n - (R_2)_{i,j-1}^n}{2\Delta y} h_{i,j}^n u_{i,j}^n \frac{v_{i+1,j}^n - v_{i-1,j}^n}{2\Delta x} \right) \\ -\frac{\Delta t}{h_{i,j}^n} \left(h_{i,j}^n v_{i,j}^n \frac{u_{i+1,j}^n - u_{i-1,j}^n}{2\Delta x} + v_{i,j}^n u_{i,j}^n \frac{h_{i+1,j}^n - h_{i-1,j}^n}{2\Delta x} + g h_{i,j}^n \frac{\partial Z}{\partial y} \right), \end{array} \tag{4.18}$$

$$\begin{array}{l} c_{i,j}^{n+1} = c_{i,j}^n - \frac{\Delta t}{h_{i,j}^n} \left(c_{i,j}^n \frac{h_{i,j}^{n+1} - h_{i,j}^n}{\Delta t} + h_{i,j}^n u_{i,j}^n \frac{c_{i+1,j}^n - C_{i-1,j}^n}{2\Delta x} \right) \\ -\frac{\Delta t}{h_{i,j}^n} \left(h_{i,j}^n c_{i,j}^n \frac{u_{i+1,j}^n - u_{i-1,j}^n}{2\Delta x} + c_{i,j}^n u_{i,j}^n \frac{h_{i+1,j}^n - h_{i-1,j}^n}{2\Delta x} + h_{i,j}^n v_{i,j}^n \frac{c_{i,j+1}^n - c_{i,j-1}^n}{2\Delta y} \right) \\ -\frac{\Delta t}{h_{i,j}^n} \left(h_{i,j}^n c_{i,j}^n \frac{v_{i,j+1}^n - v_{i,j-1}^n}{2\Delta y} + c_{i,j}^n v_{i,j}^n \frac{h_{i,j+1}^n - h_{i,j-1}^n}{2\Delta y} - c_S S \right). \end{array} \tag{4.19}$$

4.2.2 Stability analysis

We establish a result concerning the numerical stability of (4.16)-(4.19) and present its numerical implementation.

We assume that $H = max(h^n_{i,j})$, $U = max(u^n_{i,j})$ and $V = max(v^n_{i,j})$, the we have

Proposition 4.2.1 *Numerical scheme* (4.16) *is stable under the following conditions:*

$$\Delta t \leq \frac{2\Delta x \Delta y}{\Delta y(U+H) + \Delta x(V+H)}, \tag{4.20}$$

Proof. We prove it using the same procedure as in Proposition 2.3.1., this implies

$$h^n_{I,j} = \lambda^n e^{i\pi(kI+mj)}, \tag{4.21}$$

$$u^n_{I,j} = \lambda^n e^{i\pi(kI+mj)}, \tag{4.22}$$

$$u^n_{I,j} = \lambda^n e^{i\pi(kI+mj)}, \tag{4.23}$$

$$c^n_{I,j} = \lambda^n e^{i\pi(kI+mj)}, \tag{4.24}$$

with fixed constants l, k and m.

If we substitute (4.21),(4.22),(4.23) and (4.24) in (4.16) and divide by $\lambda^n e^{i\pi(kI+mj)}$, we obtain

$$\lambda = 1 - \Delta t \left((U+H)\frac{cos(\pi k)}{\Delta x} + (V+H)\frac{cos(\pi k)}{\Delta y} \right), \tag{4.25}$$

If $|\lambda| \leq 1$, numerical scheme (4.16) is stable, and thus we obtain

$$|1 - \Delta t \left((U+H)\frac{cos(\pi k)}{\Delta x} + (V+H)\frac{cos(\pi k)}{\Delta y} \right)| \leq 1, \tag{4.26}$$

this implies

$$0 \leq \Delta t \leq \frac{2\Delta x \Delta y}{\Delta y(U+H)+\Delta x(V+H)}. \tag{4.27}$$

Proposition 4.2.2 *Let a_1 and b_1, be positive constants, numerical scheme* (4.17) *is stable under the following conditions:*

$$\Delta t \leq \frac{\Delta x \Delta y(H+U)}{a_1\Delta y + b_1\Delta x + \Delta x \Delta y g z_1}, \tag{4.28}$$

such that

$$a_1 = U^2 + 2UH + gH + 2H\epsilon R_{max} + \epsilon H^2, \tag{4.29}$$

$$b_1 = HV + VU + HU. \tag{4.30}$$

with $(R_1)_{max} = max((R_1)^n_{i,j})$ and the known function $z_1 = max(\frac{\partial Z}{\partial x})$.

Proof. To prove this result, we use the same procedure as in proposition 4.2.1, we get:

$$\begin{aligned} \lambda &= 1 - \tfrac{\Delta t}{H}\left(U\tfrac{\lambda+1}{\Delta t} + U^2\tfrac{cos(\pi k)}{\Delta x} + 2UH\tfrac{cos(\pi k)}{\Delta x} + gH\tfrac{cos(\pi k)}{\Delta x}\right) \\ &- \tfrac{\Delta t}{H}\left(\epsilon H R_{max}\tfrac{cos(\pi k)}{\Delta x} + \epsilon(H)^2\tfrac{cos(\pi k)}{\Delta x} + gz_1\right) \\ &- \tfrac{\Delta t}{H}\left(HV\tfrac{cos(\pi k)}{\Delta y} + VU\tfrac{cos(\pi k)}{\Delta y} + HU\tfrac{cos(\pi k)}{\Delta y}\right). \end{aligned} \tag{4.31}$$

If $|\lambda| \leq 1$, numerical scheme (4.17) is stable, and thus we obtain

$$\left| \tfrac{H-2\Delta t}{H+U}\left(\tfrac{U^2+2UH+gH+2\epsilon H R_{max}+\epsilon H^2}{\Delta x} + gz_1 + \tfrac{HV+VU+HU}{\Delta y}\right) \right| \leq 1, \tag{4.32}$$

then, we obtain

$$\Delta t \leq \frac{\Delta x \Delta y(H+U)}{a_1\Delta y + b_1\Delta x + \Delta x \Delta y g z_1}, \tag{4.33}$$

such that a_1 and b_1 are positive constants, with

$$a_1 = max\left\{U^2 + 2UH + gH + 2H\epsilon R_{max} + \epsilon H^2\right\}, \tag{4.34}$$

$$b_1 = max\left\{HV + VU + HU\right\}. \tag{4.35}$$

Proposition 4.2.3 *Let a_2 and b_2, be positive constants, numerical scheme* (4.18) *is stable under the following conditions:*

$$\Delta t \leq \frac{\Delta x \Delta y(H+V)}{a_2\Delta x + b_2\Delta y + \Delta x\Delta y g z_2}, \tag{4.36}$$

with $(R_2)_{max} = max((R_2)^n_{i,j})$ and the known function $z_2 = max(\frac{\partial Z}{\partial y})$.

Proof. Similarly we can find that (4.36) holds, such that a_2 and b_2 are positive constants, such that

$$a_2 = max\left\{V^2 + 2VH + gH + 2H\epsilon R_{max} + \epsilon H^2\right\}, \tag{4.37}$$

$$b_2 = max\left\{HV + VU + HU\right\}. \tag{4.38}$$

Proposition 4.2.4 *Let a_3 and b_3, be positive constants, numerical scheme* (4.19) *is stable under the following conditions:*

$$\Delta t \leq \frac{\Delta x \Delta y(H+C)}{a_3\Delta x + b_3\Delta y}, \tag{4.39}$$

with $C = max(c^n_{i,j})$.

Proof. By using the same procedure, we can find that (4.39) *holds, with a_3 and b_3 are positive constants with $a_3 = max\left\{HV + VC + HC\right\}$ and $b_3 = max\left\{HU + CV + HC\right\}$.*

4.2.3 Numerical results and comment

Numerical results

To solve (4.16)-(4.19) numerically, we apply the following algorithm:

Algorithm 4.2.5

- *Step 1 (Initialization): input the gravity g, the source terms S and c_S, the bottom topography Z, the space step in both direction $(\Delta x, \Delta y)$, the time step Δt, the final time T and the initial conditions for the height h_0, the velocity (u_0, v_0) in x&y directions and the pollution concentration c_0.*
- *Step 2: solve* (4.16) *for the height h.*
- *Step 3: solve* (4.17) *for the u velocity in x direction.*
- *Step 4: solve* (4.18) *for the v velocity in y direction.*
- *Step 5: solve* (4.19) *for the pollution c.*
- *Step 6: Repeat steps $(2-5)$ until T is reached.*

The obtained Numerical results are resumed in Figures $4.1 - 4.6$ showing the variations of the flow height and the propagation of pollution in the flow at different regions.

Numerical parameters

The discretization parameters written as follows: $Lx = 10$, $Ly = 10$, $\Delta x = \Delta y = 0.3$, and the time steps $\Delta t < k \cdot CFL$ such that $k = 0.8$ and CFL is the minimum of (4.20),(4.28),(4.36) and (4.39), the gravity $g = 1$, the source terms $S = 0.1$ and $c_S = 10$

The regularized parameter ϵ is numerically adaptive $(0 < \epsilon < 1)$.

The bottom topography

$$Z(x, y) = e^{\frac{-(x-5)^2+y^2}{100}}$$

. The initial conditions for the flow height h, the velocity $U = (u, v)$ and the pollution concentration c written as follows:

$$h_0(x, y) = e^{\frac{-(x-5)^2+y^2}{100}},$$

$$u_0(x, y) = v_0(x, y) = 0,$$

$$c_0(x, y) = 2.$$

Comments on the results

- **The first numerical experimentation:**

  The obtained results are resumed in Figures $4.1 - 4.5$, showing the variation, at $t = 2$ and 3, of the flow height and the propagation of pollution for the SV-T solution (on the left of the Figures) and the RSV-T solution (on the right of the Figures), for $\epsilon = 10^{-3}$. We see that the changes are exactly in the wave curvature, which is clearly seen in the height h and velocity U in Figures 4.4 and 4.5 at time $t = 3$, where slight variances in the pollution propagation are noticed, when the wave curvature in the RSV-T is larger. Note that the results remain stable.

- **The second numerical experimentation:** If we take epsilon two times larger ($\epsilon = 2 \cdot 10^{-3}$), the stability is maintained with higher wave curvature in magnitude of h, v, u and c solutions of (4.1), see Figure 4.6.

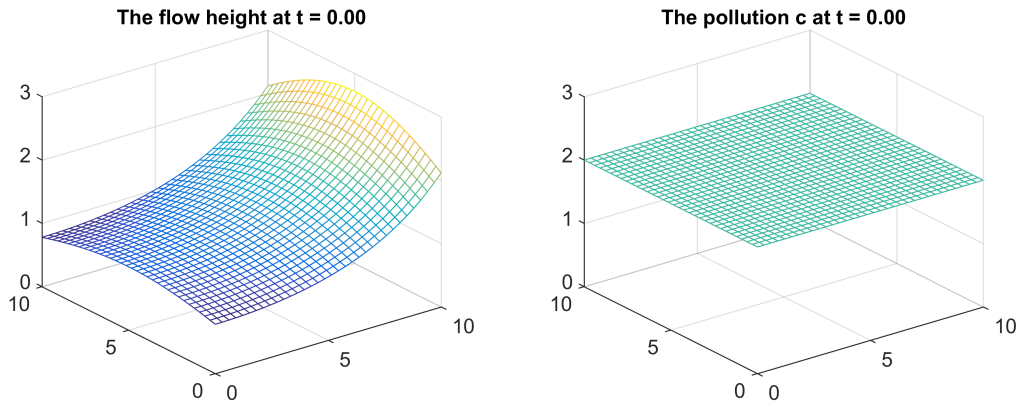

Figure 4.1: Initially the flow section for the height h and pollution c.

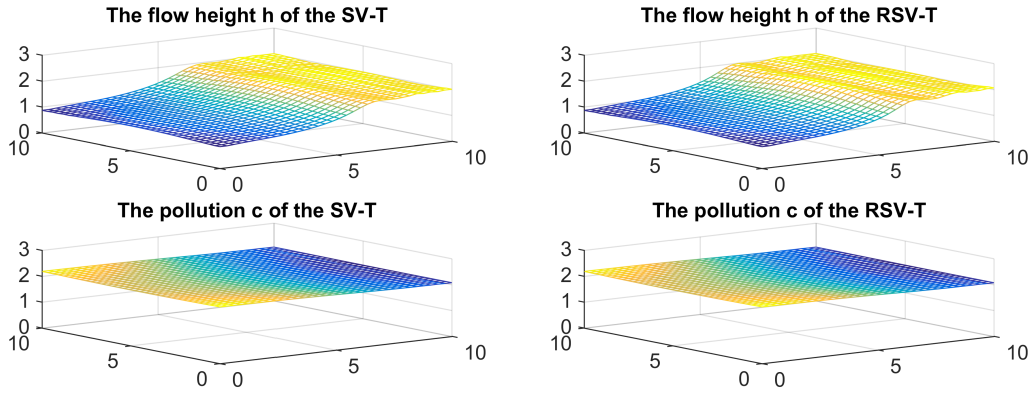

Figure 4.2: Numerical solutions for the flow height h and pollution c for both the SV-T and the RSV-T, at time $t = 2$ with $\epsilon = 10^{-3}$.

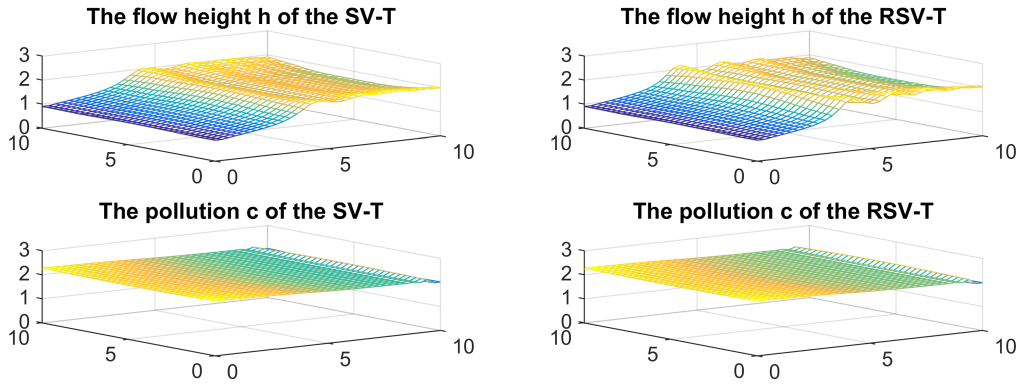

Figure 4.3: Numerical solutions of the flow height h and pollution c for the SV-T and the RSV-T, at time $t = 3$ with $\epsilon = 10^{-3}$.

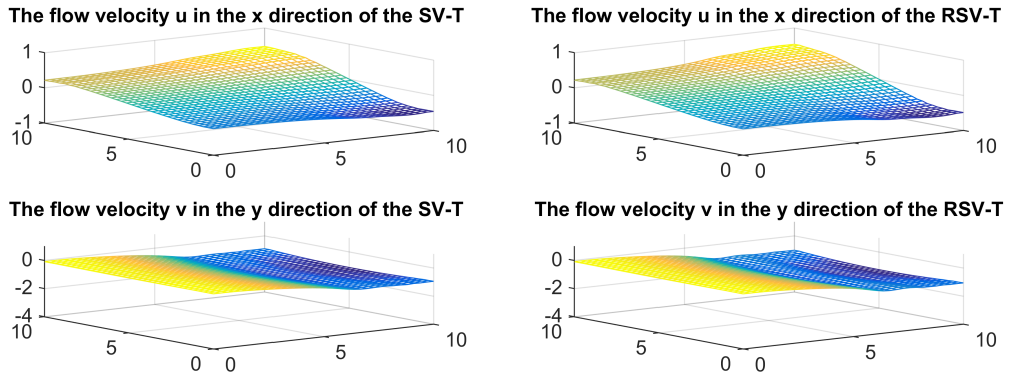

Figure 4.4: Numerical solutions of the velocity (u, v) for the SV-T and the RSV-T, at time $t = 2$ with $\epsilon = 10^{-3}$.

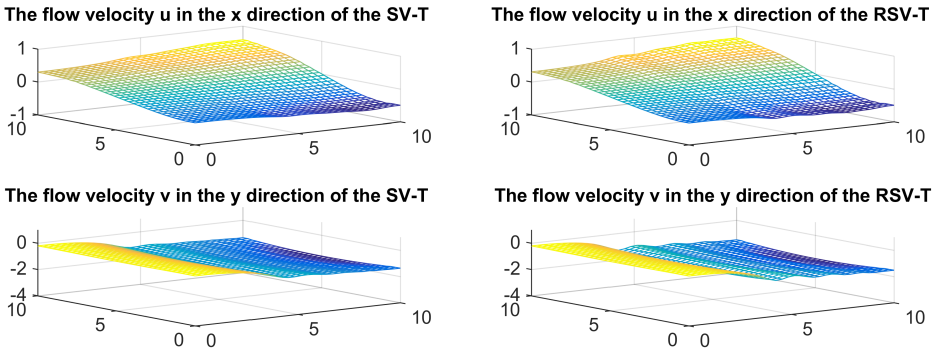

Figure 4.5: Numerical solutions of the velocity (u, v) for the SV-T and the RSV-T, at time $t = 3$ with $\epsilon = 10^{-3}$.

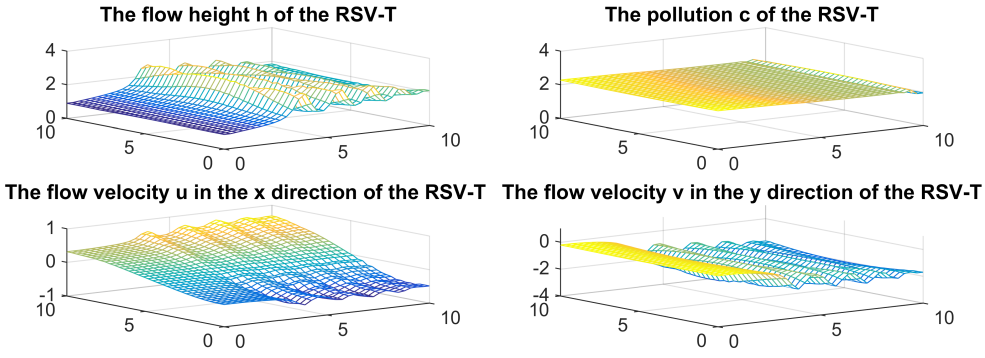

Figure 4.6: Numerical solutions of the height h, pollution c and the velocity (u, v) for the RSV-T, at time $t = 3$ with $\epsilon = 2 \cdot 10^{-3}$.

4.3 Conclusion

In this chapter, we studied the transport of a passive pollutant in a flow, using a regularisation version of SV-S coupled with a T-E. We first proved theoretical results on its well-posedness using a kinetic approach, then we focused on the numerical study of the related descretised system. In order to understand the flow height behavior and the pollutant propagation in the flow at different time and space locations, we proposed a numerical method, based on a simple explicit finite difference scheme, we derived stability conditions, so called CFL conditions ((4.20),(4.28),(4.36) and (4.39)). Different cases were studied, where the obtained results are resumed in Figures $4.1 - 4.6$. We deduct from further numerical experiments that when $\epsilon > 2 \cdot 10^{-3}$, instability occurs. Other methods of regularization can also be explored. The work of this chapter was the subject of a submitted paper.

Chapter 5

General conclusion and perspectives

In this thesis, we have studied multiple mathematical models. The first model involves a nonlinear Shallow Water Model (SWM) to comprehend flow height dynamics. The second model describes pollution propagation within the flow using a SWM, while the third model employs a regularized system of the Saint-Venant equations coupled with a Transport Equation (T-E) to analyze both the flow height and pollution spread.
Our concluding remarks are as follows:

1. In the first part of our work, a novel approach using traveling wave solutions is explored to establish the well-posedness of the SWM. Mathematical tools, namely Schauder's fixed point theorem and the Banach contraction principle were employed, then present an explicit solutions and the results are summarized in Figures $2.1-2.4$.. Numerical experiments are conducted using explicit finite difference techniques, ensuring compliance with stability conditions. Results, presented in Figures $2.5-2.7$, confirm a stability behavior.

2. The second part of our work, involves the study of the coupled SWM with T-E to analyze the pollution propagation. By employing Schauder's fixed point theorem and the Banach contraction principle, the well-posedness of the model is established, pro-

viding an explicit solutions and the results are resumed in Figures $3.1 - 3.4$. Numerical experiments that are summarized in Figures $3.5 - 3.7$, confirm stability.

3. The third part of our work focuses on the transport of a passive pollutant in a flow using a regularized version of the Saint-Venant equations. Theoretical results on well-posedness are proved, followed by a numerical study of the discretized system. A numerical method based on explicit finite difference schemes is proposed to understand the flow height behavior and pollutant propagation. Stability conditions, known as CFL conditions, are derived. The results, presented in Figures $4.1 - 4.6$, show that instability occurs when $\epsilon > 2 \times 10^{-3}$. It has to be pointed out that the parameters are chosen adaptatively.

Perspectives

The results obtained in this thesis have led to open questions regarding analysis and numerical experiments. Among these questions, we can mention, for example:

- Use of the traveling wave form in 2-D to derive theoretical results for the nonlinear model.
- Possibility of using the auto-similarity form in 1-D and 2-D for theoretical results of the nonlinear model.
- Exploration of real parameters for numerical experiments.
- The use of other models and coupling to enhance our understanding of flow height behavior and other physical phenomena.
- Application of other advanced numerical methods to obtain more accurate results.

Bibliography

[1] H. Altaie. Numerical Solutions for 2D Depth-Averaged Shallow Water Equations. International Mathematical Forum, Vol. 13, no. 2, 79-90, , 2018.

[2] A. Assala. Étude mathématique et numérique de certains problèmes des milieux poreux. Thèse de Doctorat, université Badji mokhatar annaba, 2014.

[3] A. Assala, N. Djedaidi and F. Z. Nouri. Dynamical behaviour of miscibles fluids in porous media. Int J. Dynamical Systems and Differential Equations, Vol. 8(3), 176-189, 2018.

[4] E. Audusse and M. O. Bristeau. A well-balanced positivity-preserving second-order scheme for shallow water flows on unstructured meshes. J. Comput. Phys., vlo. 206(1), 311-333, 2005.

[5] E. Audusse and M. O. Bristeau. Transport of pollutant in shallow water a two time steps kinetic method. Vol. 37, no. 2, 389-416, 2003.

[6] S. Banach. Théorie des opérations linéaires. Z Subwencji funduszu kultury Narodowej, 1979.

[7] Z. Bai and H. LU. Positive solutions for boundary value problem of nonlinear fractional differential equation. J. Math. Anal. Appl., vol 311, 495-505, 2005.

[8] N. Benhamidouche. Exact solutions to some nonlinear PDEs. travelling profiles method, Electronic Journal of Qualitative Theory of differential Equation, vol 15, 1–7, 2008.

[9] F. Benkhaldoun, I. Elmahi and M. Seaid. Well-balanced finite volume schemes for pollutant transport by shallow water equations on unstructured meshes. Journal of Computational Physics, vol 226, 180-203, 2007.

[10] O. Besson, S. Kane, and M. Sy. On a 1D-Shallow Water Model: Existence of solution and numerical simulations. Revue Africaine de Recherche en Informatique et Mathématiques Appliquées, vol 9, 247-260, 2008.

[11] F. Bousbia. Etude mathématique et numérique des équations d'onde dispersives. Thèse de Doctorat, université Badji mokhatar annaba, 2020.

[12] D. Bresch and B. Desjardins. Sur un modèle de Saint-Venant visqueux et sa limite quasigéostrophique. C.R.Acad.Paris, Ser.I, vol 335, 973-978, 2002.

[13] H. Brezis. Analyse fonctionnelle. Masson, Paris, 1983.

[14] H. S. Bhat, R. C. Fetecau and J. Goodman. A Leray-type regularization for the isentropic Euler equations. Nonlinearity, vol 20(9), 2035–2046, sep 2007.

[15] M.O. Bristeau and B. Perthame. Transport of pollutant in shallow water using kinetic schemes. ESAIM: Proceeding, URL: http://www.emath.fr/maths/proc/vol.10.

[16] L. Cai, W. Xie, J. Feng and J. Zhou. Computations of transport of pollutant in shallow water. Applied Mathematical Modelling, vol 31, 490-498, 2007.

[17] L. Camassa, R., Chiu, P.-H. and T. W. H. Sheu. Viscous and inviscid regularizations in a class of evolutionary partial differential equations. J. Comp. Phys., vol 229, 6676–6687, 2010.

[18] L. Cea and E. Bladé. A simple and efficient unstructured finite volume scheme for solving the shallow water equations in overland flow applications. Water resources research, vol 51 no. 7, 5464-5486, 2015.

[19] A. Chertock, A. Kurganov and G. Petrova. Finite-Volume-Particle Methods for Models of Transport of Pollutant in Shallow Water. Journal of Scientific Computing, Vol. 27, Nos. 1-3, June 2006.

[20] D. Clamond and D. Dutykh. Non-dispersive conservative regularisation of nonlinear shallow water (and isentropic Euler) equations. commun. Nonlinear Sci. Numer. Simul., vol 55, 237-47, 2018.

[21] R. Djemiat, B. Basti and N. Benhamidouche. Existence of traveling wave solutions for a free boundary problem of higher-order space-fractional wave equations. Appl. Math. E-Notes, 22, 427-436, 2022.

[22] D. Dutykh and D. Mitsotakis. On the relevance of the dam break problem in the context of nonlinear shallow water equations. Discrete and Continuous Dynamical Systems - Series B, vol 13(4), 799-818, 2010.

[23] F. Gerbeau and B. Perthame. Derivation of viscous Saint-Venant system for laminar shallow water. Numerical results. Discrete and Continuous Dynamical Systems-series B. 1, No. 1, 89-102, 2001.

[24] J. W. Gibbs. On the equilibrium of heterogeneous substances. American Journal of Science, vol 3, no.96, 441-458, 1878.

[25] A. Granas and J. Dugundji. Fixed Point Theory; Springer: New York. NY, USA, 2003.

[26] V. A. Isaakovich, V. Vitaly and V. Vladimir. Traveling wave solutions of parabolic systems. American Mathematical Soc., vol 140, 1994.

[27] L. Jibin, C. Guanrong and S. Jie. Bifurcations and Dynamics of Traveling Wave Solutions for the Regularized Saint-Venant Equation. International Journal of Bifurcation and Chaos, vol 30 no. 7, 2050109, 2020.

[28] S.A. Kamboh, N.S, L.Izzatul and O.E. Monday. Simulation of 2D Saint-Venant equations in open channel by using MATLAB. Journal of IT in Asia, vol 5, 2015.

[29] N. Katopodes and T. Strelkoff. Computing two-dimensional dam-break flood waves. Journal of the Hydraulics Division, ASCE , vol 104, 1269-88, 1978.

[30] H. W. Kernkamp, A. VanDam and G. Stelling and E. D. DeGoede. Efficient scheme for the shallow water equations on unstructured grids with application to the Continental Shelf. Ocean Dynamics, vol 61, 1175-1188, 2011.

[31] B. Khobalatte and P. Perthame. Maximum principle on the entropy and second-order kinetic schemes. Mathematics of Computation, vol 62, 119-131, 1994.

[32] E. Kreyszig. Introductory functional analysis with applications. Vol. 17. John Wiley and Sons, 1991.

[33] M. Lachache and F. Z. Nouri. Theoretical and numerical results for the nonlinear shallow water problem. Surveys in Mathematics and its Applications, vol 18, 2023.

[34] J. Leray. Essai sur les mouvements plans d'un fluide visqueux que limitent des parois. J. Math. Pures Appl., vol 13, 331–418, 1934.

[35] Z. Lin, Z. Liang and H. Haifeng. Traveling wave solutions of a diffusive SEIR epidemic model with nonlinear incidence rate. Taiwanese Journal of Mathematics, vol 23 no. 4, 951-980. 2019.

[36] J. L. Liu, R. L. Pego and Y. Pu. Well-posedness and derivative blow-up for a dispersionless regularized shallow water system Nonlinearity,arXiv, 1810.06096, 2019.

[37] T. Molls and M. Chaudhry. Depth averaged open channel flow model. Journal of Hydraulic Engineering, vol 121, 65-453, 1995.

[38] J. Murillo, J. Burguete, P. Brufau and P. García-Navarro. Coupling between shallow water and solute flow equations: analysis and management of source terms in 2D. International Journal for Numerical Methods in Fluids, vol 49, no.3, 267-99, 2005.

[39] C. L. Navier and G. G. Stokes. Researches on the Equations of Motion of Incompressible Fluids. Memoirs of the Royal Academy of Sciences of the Institute of France, vol. 6, 389-440, 1822.

[40] G. J. Norgard and K. Mosheni. A new potential regularization of the one-dimensional Euler and homentropic Euler equations. Multiscale Model. Simul., vol 8(4), 1212–1243, 2010.

[41] F.Z. Nouri, N. Djedaidi and S. Gasmi. Interface dynamics for a bi-phasic problem in heterogeneous porous media. Dyn. Contin. Discrete Impuls. Syst., Ser. B, Appl. Algorithms, vol 30, no. 1, 21-33, 2023.

[42] B. Perthame and C. Qiu. A Variant of Van Leers Method for Multidimensional Systems of Conservation Laws. Journal of Computational Physics, vol 112(2), 370-381, 1994.

[43] B. Perthame and C. Simeoni. A kinetic scheme for the Saint-Venant system with a source term. Calcolo, Vol 38, 201-231, 2001 .

[44] J. M. Peraud, C. D. Landon and N. G. Hadjiconstantinou. Monte Carlo methods for solving the Boltzmann transport equation. Annual Review of Heat Transfer, vol 17, 2014.

[45] Y. Pu, R.L. Pego, D. Dutykh and D. Clamond. Weakly singular shock profiles for a non-dispersive regularization of shallow-water equations. commun. Math. Sci., vol 16, 1361-78, 2018.

[46] A. J. C. Saint-Venant. Théorie du mouvement non-permanent des eaux, avec application aux crues des rivières et à l'introduction des marées dans leur lit. C. R. Acad. Sc. Paris, 73, 147-154, 1871.

[47] J. P. Sethna. Statistical mechanics: entropy, order parameters, and complexity. Vol. 14. Oxford University Press, USA, 2021.

[48] I. Siddique, K. B. Mehdi, M. M. Jaradat, A. Zaar, M. E. Elbrolosy, A. A. Elmandouh and M. Sallah. Bifurcation of some new traveling wave solutions for the time–space M-fractional MEW equation via three altered methods, Results in Physics, vol 41, 105-896, 2022.

[49] P. Sochala. Méthodes numériques pour les écoulement souterrains et couplage avec le ruissellement. Thèse de Doctorat, université Paris-Es, 2008.

[50] H. W. Streeter, and E.B. Phelps, A Study of the Pollution and Natural Purification of the Ohio River, U.S. Public Health Service Bulletin, No. 146, 1-75, 1925.

[51] S. Todorcevic. Compact sets in function spaces. In: Topics in Topology. Lecture Notes in Mathematics, vol 1652. Springer, Berlin, Heidelberg. 1997.

[52] E. F. Toro. Shock-capturing Methods for Free-surface Shallow Flows. John Wiley and Sons: Chichester, 2001.

[53] R. Touma and A.S. Mira. Finite Volume Methods for Pollutant Transport in Shallow Water Equation. AIP Conference Proceedings, Vol 2293, 030023, 2020.

[54] D. Vanzo, A. Siviglia and E. F. Toro. Pollutant transport by shallow water equations on unstructured meshes: hyperbolization of the model and numerical solution via a novel flux splitting scheme. Journal of Computational Physics, Elsevier, vol 321, 1-20, 2016.

[55] X. Wu, F. Yang and D. Liang. Study of Pollutant Transport in Environmental Flows using Depth-Averaged Random Walk Method, vol 3, 2342-2350 2018.

[56] W. Yahui, L. Guo and O. Chunhua. Speed sign of traveling waves to competitive Lotka-Volterra recursive system with bi-stable non-linearity. Communications on Pure and Applied Analysis, vol 21, no. 12, 2022.

[57] https://byjus.com/physics/fluid/